GEAR TECHNOLOGY

The Journal of Gear Manufacturing

SEPTEMBER/OCTOBER 1985

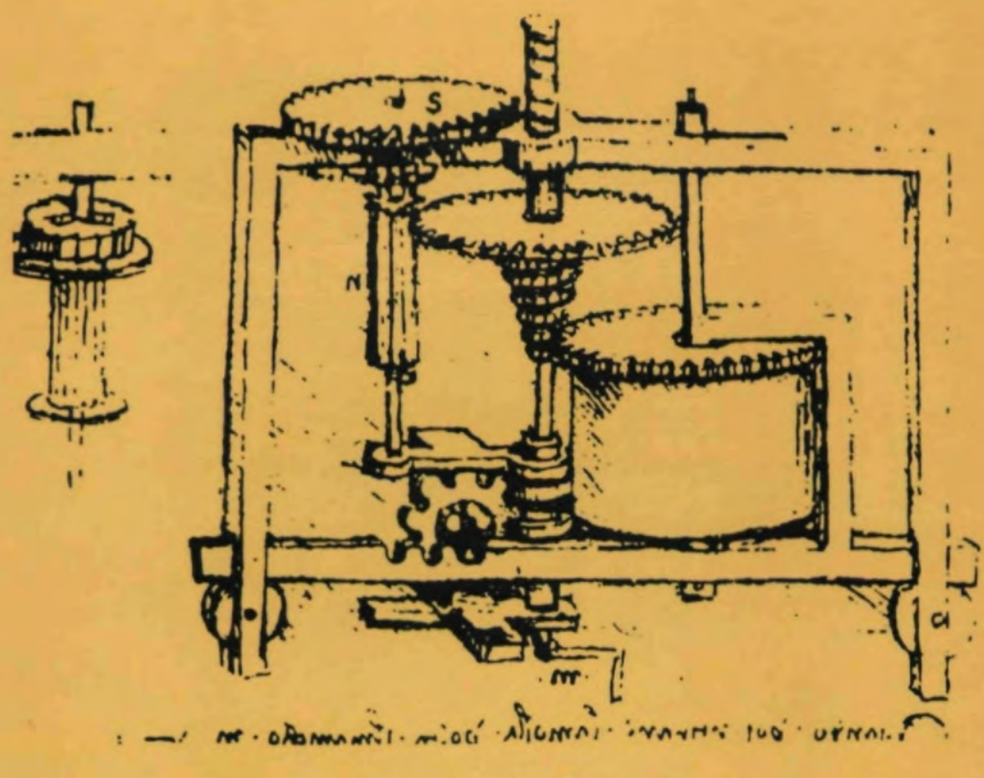

Calculation of Spur Gear Tooth Flexibility

Hob Length Effects

Single Flank Data Analysis and Interpretation

Techniques for Aligning and Maintaining Large Ring Gears

Material Selection and Heat Treatment

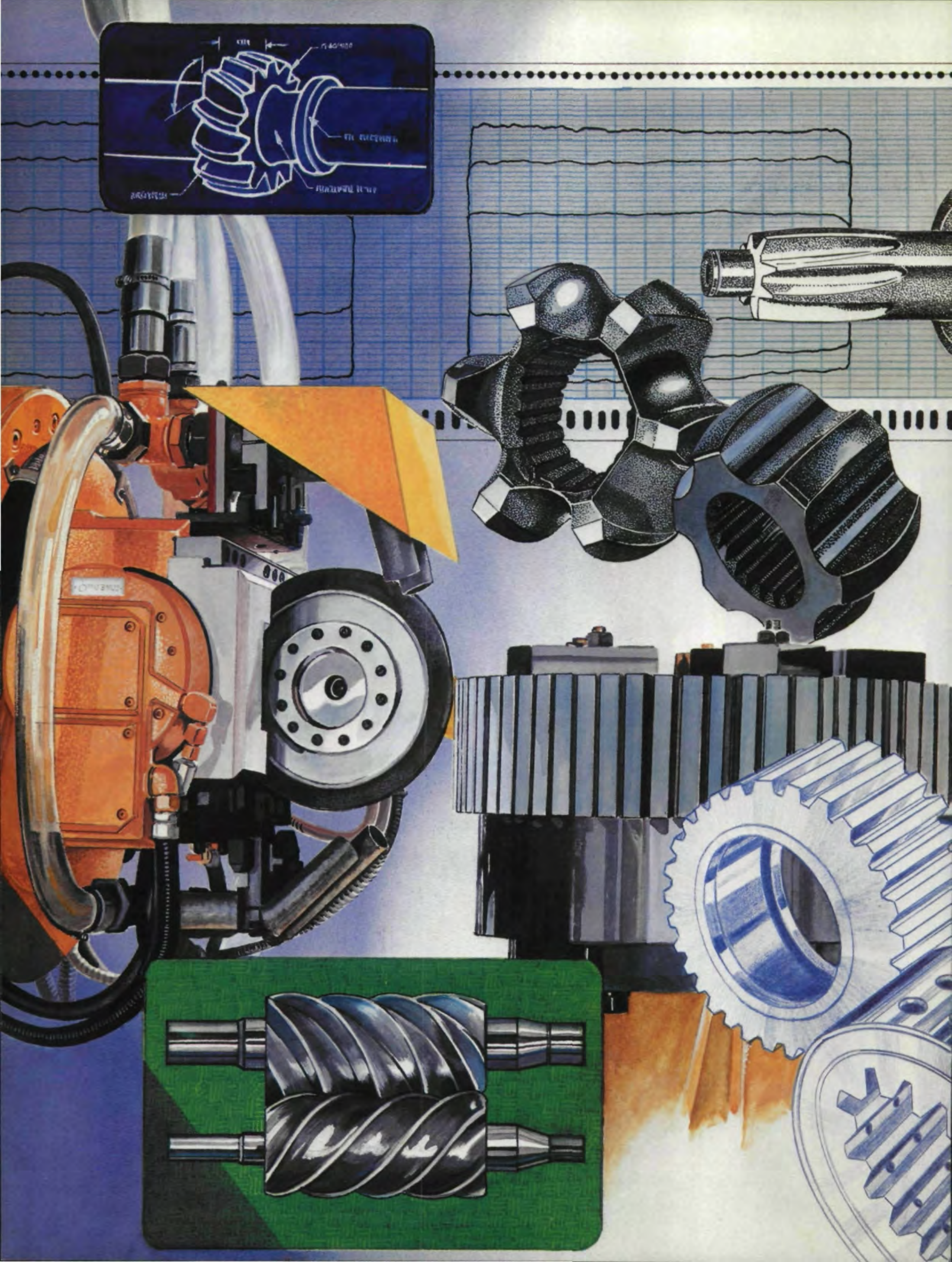

CNC hardened gear finishing, the cost-efficient technology

CNC CBN form finishing

CNC form finishing using replateable, single-layered CBN form wheels is rapidly gaining wide acceptance for mass production hard gear finishing. Specially designed CNC form grinders manufactured by Kapp and Pfauter/Kapp make this process more productive than either threaded wheel continuous generating grinding, or conventional generating grinding. It removes large envelopes of stock and, since it is free cutting, causes no burning. This process also leaves significantly lower residual stresses than vitrified grinding. Kapp and Pfauter/Kapp CNC CBN form finishing machines operate on the creep feed, deep grinding principle. They are designed for internal and external spur and helical gears, splines and non-involute shapes. Kapp and Pfauter/Kapp machines cover the complete range of gear sizes up to 4000 mm.

CNC carbide finishing

CNC finishing of hardened gears using carbide tools is no longer a research project. The process is being applied to the production of automotive transmission gears of outstanding quality, with noise and load performance rivaling ground gears...all at a lower cost-per-piece. The key to achieving these remarkable results is an equally remarkable CNC gear finishing machine. The Pfauter PF 150 is a 4-axis CNC controlled machine specifically designed for high production. It operates on the crossed axis principle to remove metal from the flanks of hardened teeth using a carbide, face sharpened cutter that moves in a shear action, progressive cut at extremely high speed.

CNC carbide finishing offers several distinct advantages. It not only corrects heat treat distortions and provides resharpening of the carbide tool on the machine, it also allows higher green gear productivity due to a larger stock envelope in precutting.

The full spectrum of gear technology

CNC hardened gear finishing is only one facet of our capability. The American Pfauter family of companies offers the complete range of modern CNC gear production technology, from individual hobbing, grinding, measuring and finishing machines...to customized flexible gear manufacturing systems for large or small lot sizes. For additional information, contact American Pfauter Ltd., 925 East Estes Avenue, Elk Grove Village, IL 60007. Phone (312) 640-7500.

AMERICAN PFAUTER

Building American Productivity

CIRCLE A-1 ON READER REPLY CARD

member national machine tool builders association

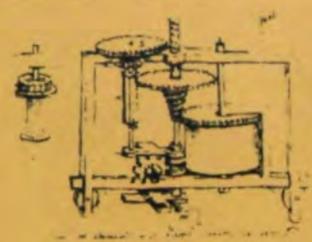

COVER

The Advanced Technology of
LEONARDO DA VINCI
1452-1519

Through Leonardo's drawings, it is possible to see him as the forerunner of the Industrial Designer. His drawings show great thoroughness and attention to technical detail. It has been possible to build perfect working models from his sketches. It seems incongruous, therefore, that although his models were feasible and could have been profitable for him, he never tried to complete his work. Yet, this seems compatible with Leonardo's character. While he had a great curiosity for everything around him, he seemed interested only in finding a solution to a problem. Once discovered, understood and resolved, he seemed to lose interest and moved on to another problem.

This month's cover sketch is a motor with gearwheels. It is one of Leonardo's studies of clock mechanisms. This device, which is more complex than his other designs, illustrates an upper rim of the spring barrel which has teeth that engage a spiral volute proportioned like a fusee. There are two screws on the axis of the volute. One has the same pitch as the sprial on the conical gear and the other actuates a worm wheel, pinion and rack to vary the position of the spring barrel. This accommodates the variable center distance required by the conical gear.

GEAR TECHNOLOGY

The Journal of Gear Manufacturing

CONTENTS — PAGE NO.

FEATURES

DEPARTMENTS

September/Octobert 1985 — Vol. 2, No. 5

GEAR TECHNOLOGY, The Journal of Gear Manufacturing (ISSN 0743-6858) is published bimonthly by Randall Publishing Co., Inc., 1425 Lunt Avenue, P. O. Box 1426, Elk Grove Village, IL 60007. GEAR TECHNOLOGY, The Journal of Gear Manufacturing is distributed free of charge to qualified individuals and firms in the gear manufacturing industry. Subscription rates for non-qualified individuals and firms are: $30.00 in the United States, $50.00 for foreign countries. Application to mail at second class postage rate is pending at Arlington Heights, IL, and at additional mailing office.

Postmaster: Send address changes to GEAR TECHNOLOGY, The Journal of Gear Manufacturing, 1425 Lunt Avenue, P. O. Box 1426, Elk Grove Village, IL 60007.

MANUSCRIPTS: We are requesting technical papers of every sort from manufacturers of gear making machinery and related equipment, universities, and engineers. Articles should be of an educational and training nature with general appeal to anyone having anything to do with the purchase of materials or machinery, or the design, manufacture, testing or processing of gears. Subjects sought are solutions to specific problems, explanations of new: technology, techniques, designs, processes, and alternative manufacturing methods. These can range from the "How to . . ." of gear cutting (**BACK TO BASICS**) to the most advanced technology. All manuscripts submitted will be carefully considered. However, the Publisher assumes no responsibility for the safety or return of manuscripts. Manuscripts must be accompanied by a self-addressed, self-stamped envelope, and be sent to GEAR TECHNOLOGY, The Journal of Gear Manufacturing, P.O. Box 1426, Elk Grove, IL 60007, (312) 437-6604.

NOTES FROM THE EDITOR'S DESK

While on holiday in England during July, my thoughts for this page were on the proposed changes to our tax law, and how they would adversely affect America's industry. But with the President undergoing cancer surgery, Congress deadlocked on deficit reduction and the budget on the back burner, nothing new was being said or done regarding a new tax law. Therefore, with nothing of import to our industry to reflect upon, I decided to share an experience that I thought would be of interest.

A few years ago, an English friend of mine, Iain Exeter, bought a company called B.L.E. Engineering, manufacturer of modified and racing versions of Jaguar automobiles, known as Lister Jaguars. During my visit, he secured a racing track at Bruntingthorpe for some of his friends and customers, and for my wife and me to put some cars through their paces, under simulated semi-race conditions.

The day was atypical in every way, from the clear blue skies and sunshine (remember, this was in England) to the startling array of motorcars: an XJ13 Style Invicta Racer, powered by a 5.7 liter V12 440HP engine with 6 dual downdraft Webbers sitting behind the driver, driven through a Z-F transaxle; a Jaguar XJS Lister Racer with a 5.7 liter 400HP engine, which was to race the next day at Donnington; a 5.7 XKE Lister with 6 dual downdraft Webbers; a TVR 350i, (a fast and beautiful car which we don't see in the U.S.); a Ferrari 512BB Boxer and other, more "normal" cars.

For about six hours we roared around the track, trying to push these cars to their limit. I did some circuits in the Invicta with Roger Mac, the celebrated race driver at the wheel, to get an idea of what the limit is really like:

Iain Exeter and M. G. with XJ Lister Racer

unbearable heat, the smell of burning rubber, the deafening roar of the engine, and the tires operating at the limit of their ability to stick to the ground — exhilarating! Iain's son Tim lost control of the XJS Racer, with me as a passenger, and we wound up in a wheat field, but fortunately there were no serious injuries.

Dr. Pooler and the boys at Ford have their Cobras, the guys at Chevy their 'Vettes, and Chrysler their muscle cars, but it's a rare opportunity to drive some of Europe's exotica.

Good fun was had by everyone — a most enjoyable and unforgettable day. Thanks, Iain!

Marsha Goldstein driving the XJ13 Invicta

Michael Goldstein
Editor/Publisher

INDUSTRY FORUM

"INDUSTRY FORUM" provides an opportunity for readers to discuss problems and questions facing our industry.

Please address your questions and answers to: INDUSTRY DISCUSSION, GEAR TECHNOLOGY, P.O. Box 1426, Elk Grove Village, IL 60007.

Letters submitted to this column become the property of GEAR TECHNOLOGY. Names will be withheld upon request; however, no anonymous letters will be published. Opinions expressed by contributors are not necessarily those of the editor or publishing staff.

Dear Editor:

Your May/June issue contains a letter from Edward Ubert of Rockwell International with some serious questions about specifying and measuring tooth thickness. AGMA is working on a new standard (AGMA 231.XX) which addresses these problems in more detail than anything now in print. Because this is a working draft and not a published standard, it is not yet available for general distribution. The committee is reviewing the document, and it will probably reach the "committee comment" stage this year. If Mr. Ubert would like to review the document and make comments on it, he should contact AGMA.

I suspect that the discrepancy which he encounters in using pins to check gears with low numbers of teeth and high helix angles is a function of the pins rocking in the mesh as he makes his measurement. It is generally better to use balls for measuring helicals since pin measurements are hard to reproduce.

Another possible source of problems is in the use of measurement over two pins to determine backlash. Since backlash is a function of runout and center distance as well as tooth thickness, and runout problems are not shown by a two pin measurement, it is conceivable that the radius over one pin or ball would give Mr. Ubert more reliable results.

Addendum modifications can be used on any gear set. They merely affect the operating center distance, not the interchangeability. All gears of the set will be interchangeable if they have the same normal base pitch and base helix angle.

This subject is very long and complicated. There is not complete agreement on the best ways to do these measurements, although everyone agrees on the mathematics. The effects of gear quality variation (lead, profile, pitch and runout) on tooth measurement are the whole subject of the new AGMA standard and can't be covered in one letter.

Don McVittie
The Gear Works
Seattle, Washington 98108

Now you can have quality-assured master gages through our computerized gear and spline QC system

Master gears which remain constant for years

Now M & M Precision Systems offers complete designing and manufacturing of master gears used in all types of gear inspection procedures... setting, rolling and sizing masters—spur and helical. Accuracy levels required for master reference, QC inspection or production grades are assured through testing with our computer-controlled Model 2000 QC System—the industry standard for automated gear and spline testing.

Shown above is the 2000 QC system at work checking a master gear. The blow up at the right shows the simple system transducer scanning a master gear for true universal gear inspection. Also shown is a printout of an involute check made under total computer control.

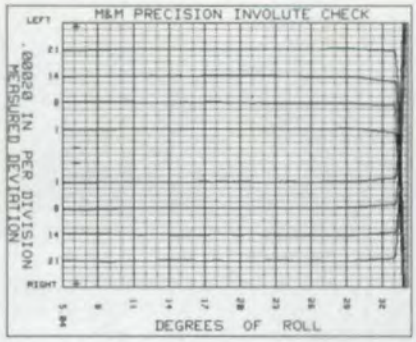

Strict, automated quality control is inherent in every manufacturing stage and, upon part completion, every aspect of material stability and dimensional accuracy is checked again so that our master gears will give you years of constant service. Before shipping, individual product records of every product are reviewed and certified. Calibration certificates, traceable to the National Bureau of Standards are supplied.

We also make quality-assured spline gages

Our plug gages and ring gages are manufactured under the same strict inspection procedures as our master gears. We make setting, alignment, and GO/NO GO masters in a variety of configurations such as sector, involute, serrated, tapered, and helical.

Other related products now available include:

- Comparators
- Rotolock Arbors
- Master Worms
- Helical Spline Plugs and Rings
- Index Plates
- Broaching Rings

For quotations or applications information, write or call M & M Precision Systems, 300 Progress Rd, West Carrollton, OH 45449, (513) 859-8273. Ask for our *QC Master Gage* brochure.

M&M PRECISION SYSTEMS

AN ACME-CLEVELAND COMPANY

CIRCLE A-6 ON READER REPLY CARD

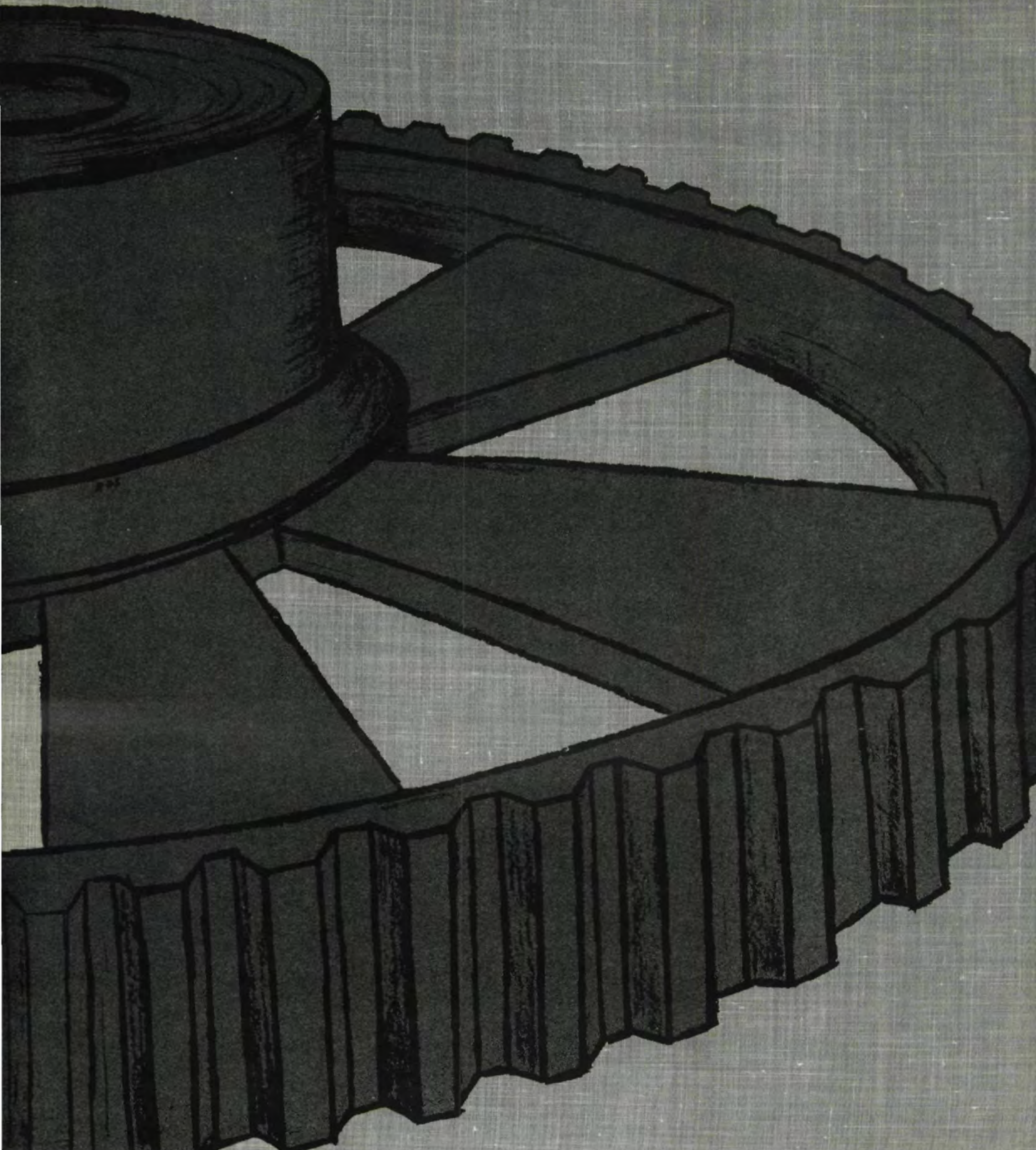

Calculation of Spur Gear Tooth Flexibility by the Complex Potential Method

A. Cardou
G. V. Tordion
Dept. of Mechanical Engineering, Laval University
Quebec, P.Q., Canada G1K7P4

Introduction

Calculation of gear tooth flexibility is of interest for at least two reasons: (a) It controls, at least in part, the vibratory properties of a transmission system hence, fatigue resistance and noise; (b) it controls load sharing in multiple tooth contact.

Earlier works on that subject are by Walker[1,2] and by Weber,[3] from the experimental and analytical point of view, respectively. More recently, the finite element method has been used,[7,9] as well as a modified beam theory.[10]

The Complex Potential Method (CPM), based on the conformal mapping of a tooth profile onto the half plane, is another interesting approach in that it provides analytical expressions for stresses and displacements. The accuracy of the results thus obtained depends only on the accuracy of the conformal transformation. Details on the CPM method can be found elsewhere.[6,11]

Calculation of tooth flexibility by the Complex Potential Method has already been presented by Premilhat et al.[8] However, two difficulties were pointed out in that paper, which do not occur in stress calculations: (a) the indeterminacy of the displacements; (b) the singularity at the point of interest, that is the teeth contact point. The first problem was not addressed in reference,[8] while the second was circumvented by calculating deflections on the tooth axis instead of at the contact point, thus losing the effect of local compression. The present paper is an attempt to show how these two problems can be dealt with in order to obtain a more accurate value of tooth flexibility at each point of the line of action for a given pair of spur gears. Detailed calculations can be found in reference.[13]

AUTHORS:

MR. ALAIN CARDOU *is a professor of mechanical engineering at Laval University, Quebec City, Canada. Dr. Cardou received his BS from Ecole Nationale Supérieure de Mécanique, France, and his MS and PhD from the University of Minnesota, in the area of Mechanics and Materials. He is conducting research on the stress and strength analysis of various mechanical elements. He is a member of ASME.*

MR. GEORGES V. TORDION *is a professor of mechanical engineering at Laval University, Quebec City, Canada. After receiving his engineering degree from the Swiss Federal Institute of Technology in Zurich, he worked for the Escher-Wyss Co., Zurich. He became a mechanical engineering professor at the Zurich State College of Engineering in Winterthur and, later, at Laval University. His main research interest has always been in gear technology: kinematics, dynamics, strength, production, lubrication. He is a member of ASME and academic member of AGMA. In 1983, he received the AGMA "Edward P. Connell" Award in recognition of his contribution to the advanced gear research and engineering education. He is a member of IFToMM (International Federation for the Theory of Machines and Mechanisms), and the French language editor of the Journal of Machines and Mechanisms.*

Basic Displacement Equations

It has been shown[11] that, for one tooth protruding out of a half plane, and subjected to a concentrated normal force W (Fig. 1), displacements u and v are given by:

$$2\mu(u+iv)=\kappa\phi(\zeta)-\frac{\omega(\zeta)}{\bar{\omega}'(\bar{\zeta})}\phi'(\zeta)-\bar{\psi}(\zeta) \tag{1}$$

where $w(\zeta)$ is the conformal mapping of the tooth profile:

$$z=\omega(\zeta)=c\zeta+\sum_{k=1}^{n}\frac{a_k}{\zeta-ib_k} \tag{2}$$

and the potentials $\phi(\zeta)$ and $\psi(\zeta)$ are given by:

$$\phi(\zeta)=-\frac{W}{2\pi}e^{i\alpha}\log(\zeta-\zeta_o)-\sum_{k=1}^{n}\frac{a_k}{\zeta-ib_k}\cdot\frac{\bar{\phi}'(ib_k)}{\bar{\omega}'(ib_k)} \tag{3}$$

$$\psi(\zeta)=\frac{W}{2\pi}e^{-i\alpha}\log(\zeta-\zeta_o)-\frac{\bar{\omega}(\zeta)}{\bar{\omega}'(\zeta)}\phi'(\zeta)+$$

$$+\sum_{k=1}^{n}\frac{a_k}{\zeta+ib_k}\frac{\phi(-ib_k)}{\omega'(-ib_k)} \tag{4}$$

Coordinates (x, y) in the z-plane are in inches, that is, they correspond to a diametral pitch $P = 1$. For any other pitch, one should multiply them by $1/P$. The same remark applies to the various figures of this paper.

Parameters c, a_k, b_k ($k = 1, 2, \ldots, n$) have to be calculated for each given profile. Once they are known, one sees that displacements u and v can be obtained from equation

Table 1 Conformal mapping parameters: standard AGMA profile (20 teeth, 20 deg)

k	a_k	$b_{(k)}$
1	0.249242305	0.435215176
2	0.101283187	0.099594373
3	0.011811730	0.020010559
4	0.001711074	0.004242494
	$c = 0.946769291$	

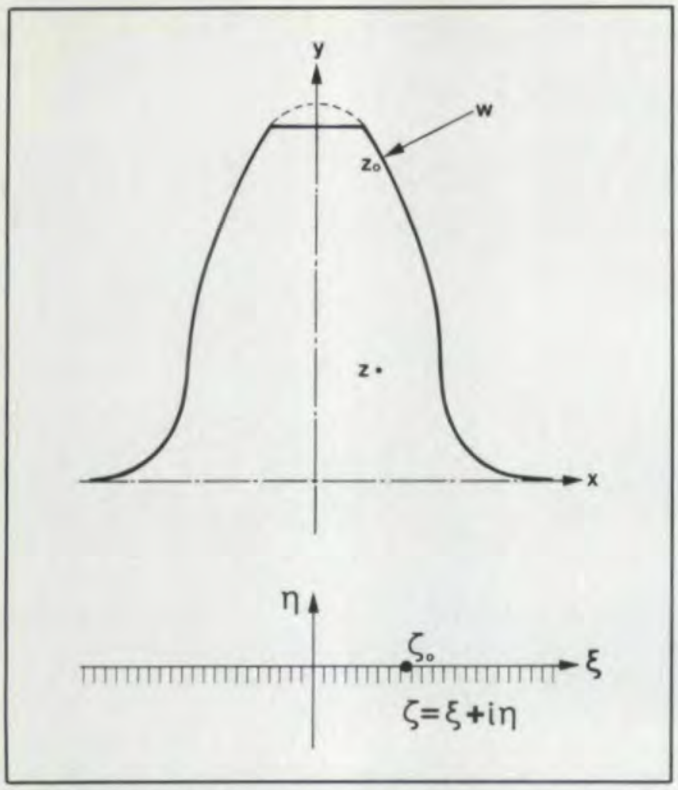

Fig. 1—Conformal mapping of a spur gear tooth.

(1). As an example, transformation parameters for a standard AGMA profile (20 teeth, 20 deg pressure angle) are given in Table 1. Explicit formulas yielding u and v in terms of these parameters have already been reported by Cardou and Tordion[11] and are much too cumbersome to be repeated here.

However, potentials $\phi(\zeta)$ and $w(\zeta)$, and thus u and v, are defined within an arbitrary constant. Besides, the elastic domain being semi-infinite, they are unbounded as z (or ζ) tends to infinity. However, for large enough z, ϕ and ψ are equivalent to their log $(\zeta - \zeta_o)$ term, showing that u and v increase very slowly. Finally u and v are singular for $\zeta = \zeta_o$, that is near the loading point.

Indeterminacy of Displacements

Although a minor problem from the mathematical point of view, indeterminacy of displacements cannot be treated lightly for practical applications. Indeed, a shift in the displacements yields a corresponding increase or decrease of the tooth flexibility. If one compares the displacements or flexibility curves published by various authors, (see, for example reference),[9] one notices that, although very similar in shape, they appear shifted from one another; the shifts are so large that one can get values differing by more than 100 percent for a given tooth.

The way to eliminate the arbitrary constants is to select a reference point and subtract its displacements from those obtained at the point of interest with the same formulae. Alternatively, an equivalent approach is to define a point as fixed in the solid. The disagreement between published displacement curves seems to come mainly from the selection of a reference point (or of a fixed boundary).

It is shown in Fig. 2 how nondimensional displacements **u** and **v** vary along the axis of a standard tooth under tip loading. For example, if one takes the reference point on the axis, at $3.4/P$ from the pitch circle, the displacement **u** at the tip is 15.3. At $5.4/P$ it is 15.6, and at $7.5/P$ it is 15.7, a variation of less than 1 percent. Thus, it is important to select the reference point deep enough. However, beyond a certain depth, displacements vary very slowly. For thin rim gears, the reference point should of course, be chosen within the rim (and rim deformation should be taken into account separately).

In the following study, the reference point is taken on the tooth axis at twice the tooth height under the root circle. For a standard AGMA profile, this corresponds to a depth of $4.5/P$ from the root circle or $5.75/P$ from the pitch circle.

Displacements at the Contact Point

In order to obtain the flexibility of a given pair of mating teeth, one has to obtain the displacement component of the contact point in the direction of the line of action. However, as mentioned earlier, equations (1) to (4) have been obtained for a concentrated load W, which makes these equations singular precisely at the contact point. Three approaches may be considered to avoid that problem:

(a) Calculate the displacements on the line of action at a given depth under the surface. This approach has been used in reference,[8] where the selected point is the in-

Fig. 2—Tooth axis displacements for tip loading (Standard AGMA profile, 20 teeth, 20 deg).

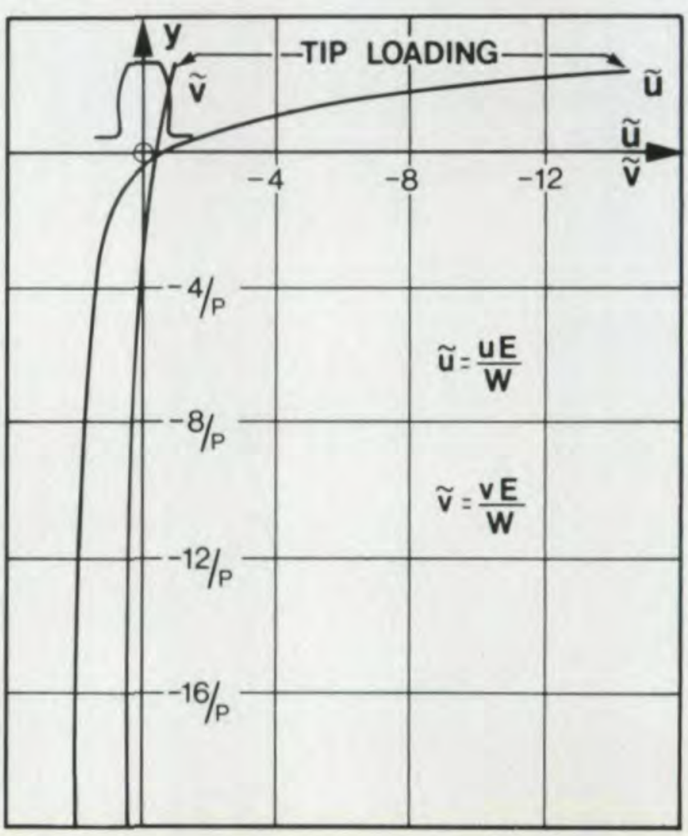

tersection between tooth axis and line of action. By doing so, one loses the local pressure displacements.

(b) Instead of a concentrated load, take a distributed one and recalculate the potentials. This is, of course, the mathematically exact approach. However, it leads to very cumbersome calculations only to get a correct displacement field near the load. Moreover, these expressions depend in a nonlinear fashion on the pair of mating gears, and on the load transmitted.

(c) Utilize the point load solution and correct it near the point of contact. In this approach, one considers that in the immediate neighborhood of that point, displacements behave in the same fashion as for a half plane under the same type of load, either concentrated or distributed. It is indeed possible, in this case, to establish a relationship between the two types of solution and apply it to the tooth problem. This is shown in the following.

Displacements for points on the line of action, calculated with the point load solution are shown in Fig. 3, for three locations of the contact point. It appears that the shape of the curves for points near the surface are almost identical, thus showing that the displacement gradient at those points is independent of the shape of the solids in contact. This leads us to the half-plane problem.

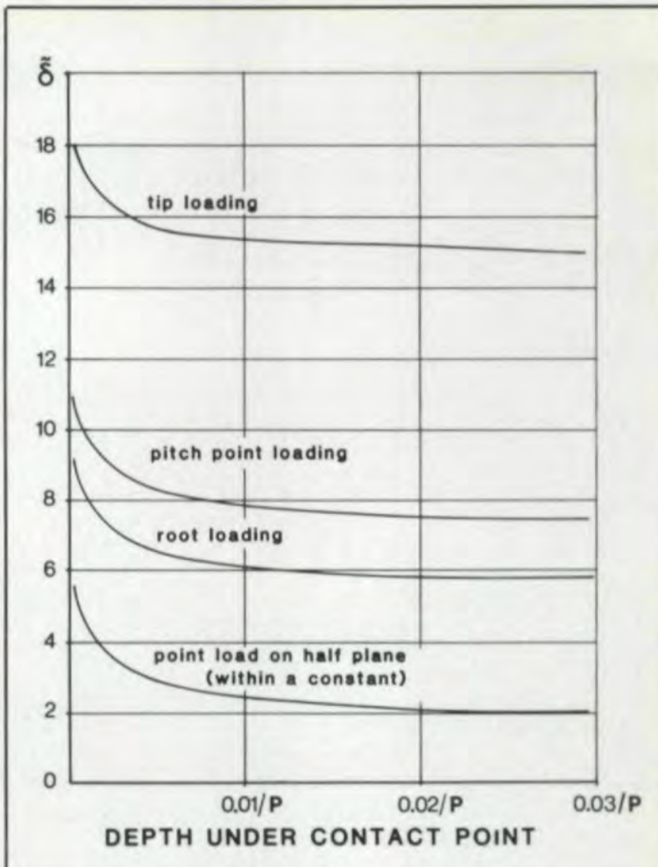

Fig. 3 – Displacement $\bar{\delta}$ of points located on the line of action versus depth under the surface; point load at tip, pitch point, and root of tooth; comparison with corresponding half-plane solution.

The Half-Plane Solutions

Nondimensional displacement $\mathbf{v}_{P_o}$ on the axis of a normal load W acting on a half plane is given, within a constant, by:

$$\mathbf{v}_{P_o} = \mathbf{v}_P(0,y) = \frac{2(1-\nu^2)}{\pi}\log|y| - \frac{1+\nu}{2\pi} \tag{5}$$

Now, consider an elliptic pressure p (Fig. 4):

$$p = \frac{2W}{\pi b^2}\sqrt{b^2-x^2} \tag{6}$$

such that

$$W = \frac{\pi b\, p_{max}}{2} \tag{7}$$

Using Westergaard's potentials,[5] one finds the corresponding displacement of a Hertz elliptical distribution load, within a constant, as:

$$\mathbf{v}_{H_o} = -\frac{2(1-\nu^2)}{\pi}\log\left[\frac{y}{b}+\sqrt{1+\left(\frac{y}{b}\right)^2}\right] + \frac{2\nu(1+\nu)}{\pi}\,\frac{y}{b}\left[\sqrt{1+\left(\frac{y}{b}\right)^2}+\frac{y}{b}\right]+C \tag{8}$$

Nomenclature

a_k, b_k, c = conformal mapping parameters
b = width of contact zone
C = arbitrary constant
E = Young's modulus
h = depth under the contact point for equivalent displacement calculation
i = imaginary constant $i = \sqrt{-1}$
p = contact pressure
P = diametral pitch
u,v = displacements in x, y directions, respectively
v_H = displacement corresponding to an elliptically distributed load (Hertz' theory)
v_P = displacement corresponding to a point load
v_{H_o}, v_{P_o} = displacements along y-axis at $x = 0$
W = normal load/width
x,y = z-plane coordinates (diametral pitch $P = 1$)
z = defines the location of any material point in the plane $z = x + iy$
z_o = location of contact point in the z-plane
β = angle between x-axis and line of action (W)
δ = displacement of points of the line of action in its direction
δ_o = displacement of contact point
ζ = location of a material point in the conformally transformed plane $\zeta = \xi + i\eta$
k = material constant $k = 3 - 4v$
v = Poisson's ratio
μ = Lamés parameter $\mu = E/2\,(1 + v)$
μ,ξ = ζ-plane coordinates
φ,ψ = complex potentials
ω = conformal mapping function, $z = \omega(\zeta)$
$\bar{z},\bar{y},\bar{\varphi},\bar{\psi}$ = complex conjugates of corresponding functions
$\mathbf{v},\bar{\delta}$ = nondimensional displacements $v = uE/W$ $\delta = \delta E/W$

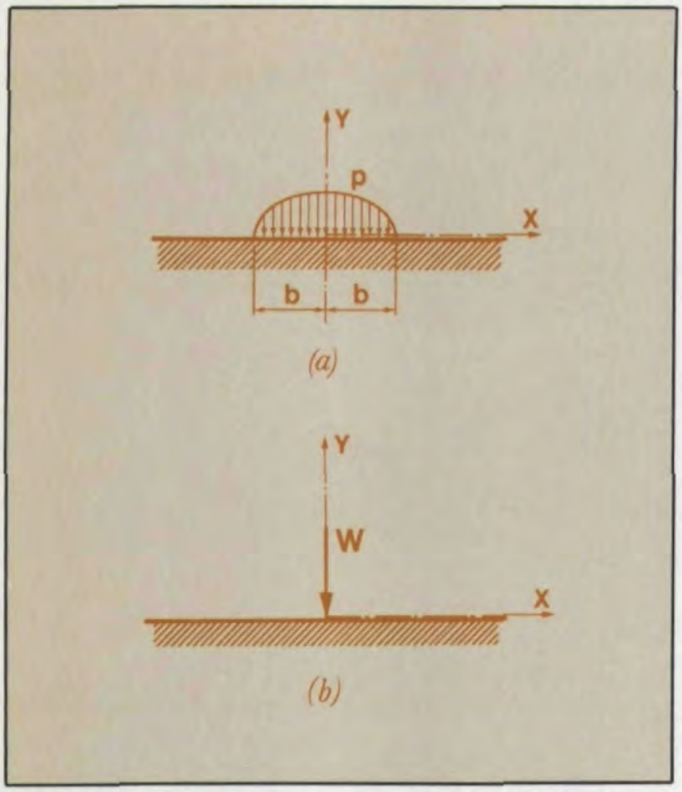

Fig. 4—Half-plane cases: (a) elliptically distributed load (b) point load.

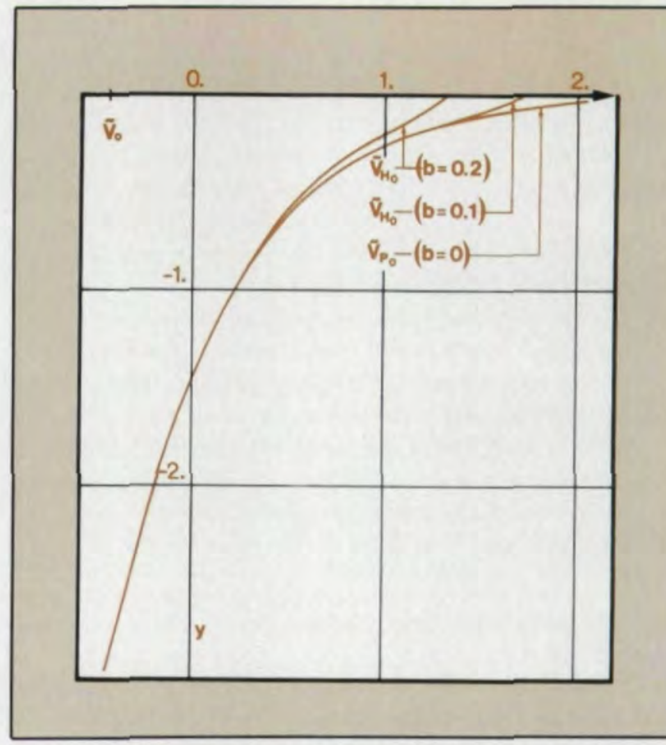

Fig. 5—Half-plane solutions: comparison of displacements $\tilde{v}_{H_o}$ (b = 0.1, 0.2) and $\tilde{v}_{P_o}$ (b = 0).

Obviously, far enough from the boundary, solution (8) should converge to solution (5). Thus, letting y tend to $-\infty$ in equation (8) and comparing with equation (5) yields the constant C:

$$C = \frac{1+\nu}{\pi}\left[2(1-\nu)\log\frac{b}{2} + \nu - \frac{1}{2}\right] \tag{9}$$

Thus, in the case of the elliptic load, displacement at the boundary point $x = y = 0$ is obtained from equations (8) and (9):

$$\mathbf{v}_{H_o}(0) = C = \frac{1+\nu}{\pi}\left[2(1-\nu)\log\frac{b}{2} + \nu - \frac{1}{2}\right] \tag{10}$$

Typical curves $\mathbf{v}_{P_o}$ and $\mathbf{v}_{H_o}$ are represented in Fig. 5. One sees that, at certain depth y_o under the surface (Fig. 6):

$$\mathbf{v}_{H_o}(0) = \mathbf{v}_{P_o}(y_o) \tag{11}$$

Letting $h = |y_o|$, this relation yields:

$$h = \frac{b}{2}\, e^{\nu/2(1-\nu)} \tag{12}$$

a simple linear relationship between h and b. For example for v = 0.3:

$$h = 0.6195\, b \tag{13}$$

Thus, considering that, in the immediate neighborhood of the contact point, relative displacement solutions are practically identical for the tooth and half-plane problems, equation (12) allows one to use the point-load solution to calculate displacements at a distance h below the surface, on the line of action. These displacements are then equal to those arising from an elliptically distributed load. Parameter b has to be calculated using the classical Hertz formulas[14] and will depend on the mating gears (size and material), on the load transmitted, and on the location on the line of action, since profile curvature varies from point to point.

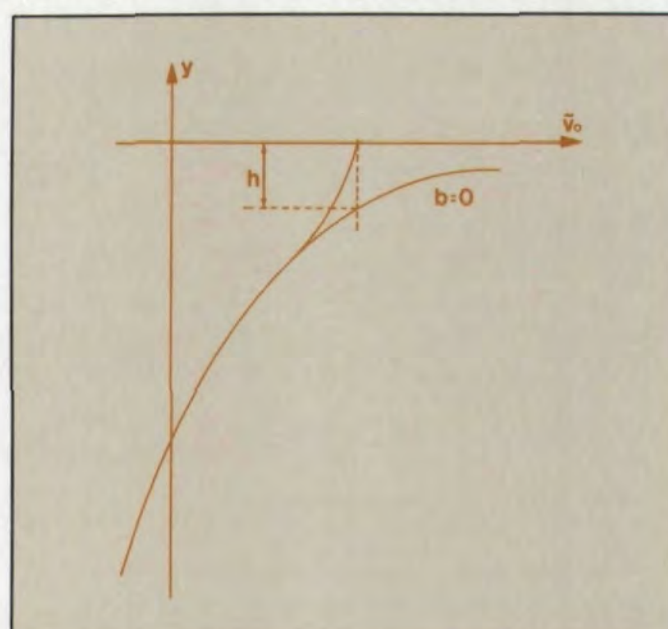

Fig. 6—Equivalent depth h for surface displacement calculation.

Calculation of Tooth Flexibility

Fig. 7 shows nondimensional displacement curves δ_o calculated for a standard AGMA profile (30 teeth, 20 deg) as a function of the contact point abscissa on the line of action and for depths h = 0.0015 in., 0.01 in., 0.1 in. under

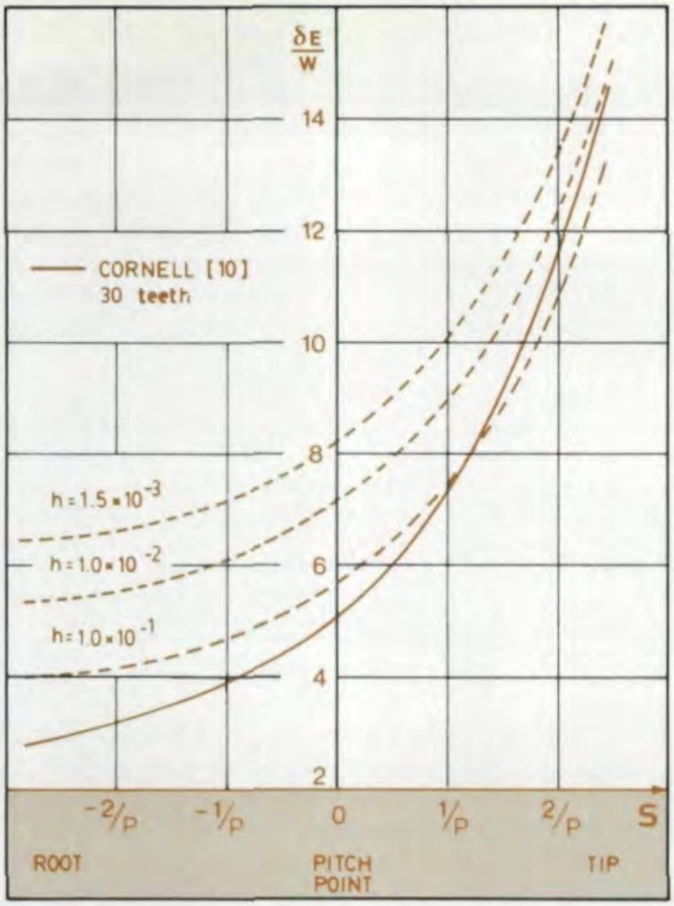

Fig. 7 – Displacement $\bar{\delta}_0$ versus abscissa of load on line of action; standard AGMA gear (30 teeth, 20 deg); calculation depths: h = 0.0015 in., 0.01 in., 0.1 in. under contact point

the surface. It is important to note that these curves are independent of the absolute dimensions of the gear. The flexibility curve obtained by Cornell[10] for the same profile is also shown in Fig. 7. It does not include the local deformation since that deformation would depend on the mating gears geometry, as well as on materials and transmitted loads.

Indeed, for a given pair of gears, and a given tangential load W, one has to calculate the corresponding depth of calculation h at each loading point. The resulting flexibility curve is shown in Fig. 8 for the particular case of a pair of identical standard AGMA gears with the following characteristics:

number of teeth:	20
pressure angle:	20 deg
pitch P:	1
material:	steel
pressure at pitch point:	200 MPa

Besides, if the contact ratio is taken into account, there is a decrease in the load W when two pairs are in contact. Paradoxically, the flexibility curves seems to indicate a slightly higher nominal deflection in that case than when only one pair is in contact. This is due to the fact that, for a given pressure at pitch point, contact pressure is lower in the double contact region, yielding a smaller contact width b, and a smaller depth h. Thus, nondimensional flexibility curves $\boldsymbol{\delta}_o = \delta E/W$ are discontinuous between single and double contact regions, owing to the fact that contact pressure is nonlinearly related to W.

In the load-sharing case, one should calculate deflections iteratively since pairs of gears, at a given instant, have a different flexibility. Thus to know how they share the total load W, one has to know the flexibility curve.

That effect on nondimensional displacement $\boldsymbol{\delta}_o = \delta_o E/W$ is due mainly to the Hertz effect (local compression), which varies as $W^{1/2}$, and it is easily verified that very little discrepancy is obtained on the nondimensional flexibility curve by letting each pair in contact share the load equally. The approximate curve thus obtained can then be used to calculate the real distribution.

Finally, the global flexibility curve for a given pair of gears is obtained by adding the separate curves for each gear. Fig. 9 shows the case of a pair of identical standard AGMA gears with indicated parameters. The CPM flexibility curve is compared with that obtained using Weber's approach. In this case, agreement is quite good except for a shift of one curve with with respect to the other, due to a different way of selecting a reference point.

Conclusion

It has been shown how expressions obtained through CPM, in the point load case, can be used to calculate displacements at the contact point of a given pair of spur gears. First, a proper reference point has to be selected; then, displacements have to be calculated at a certain depth under the surface. That depth has been shown to vary linearly with the width

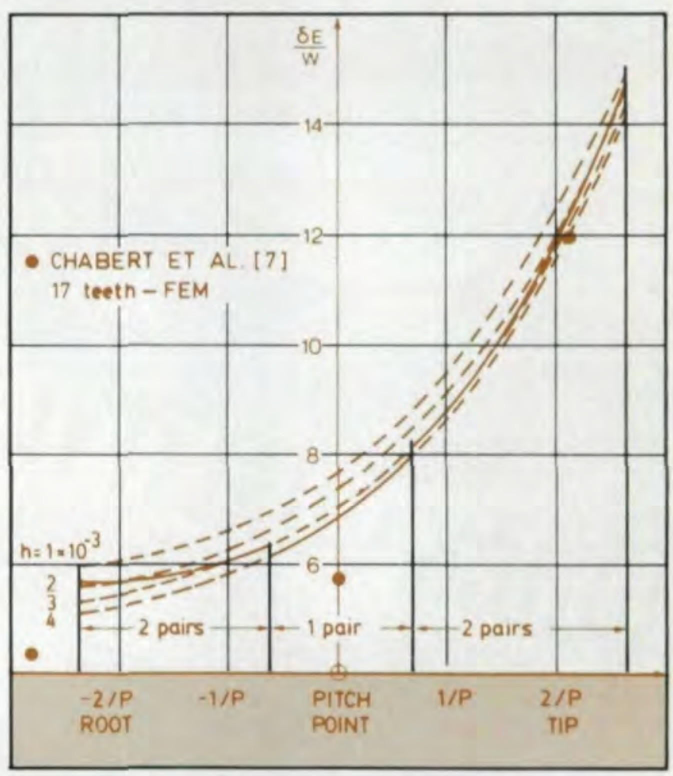

Fig. 8 – Displacement $\bar{\delta}_0$ versus abscissa of load on line of action for a standard AGMA gear (20 teeth, 20 deg) meshing with an identical gear; maximum pressure at pitch point: 200 MPa, P = 1.

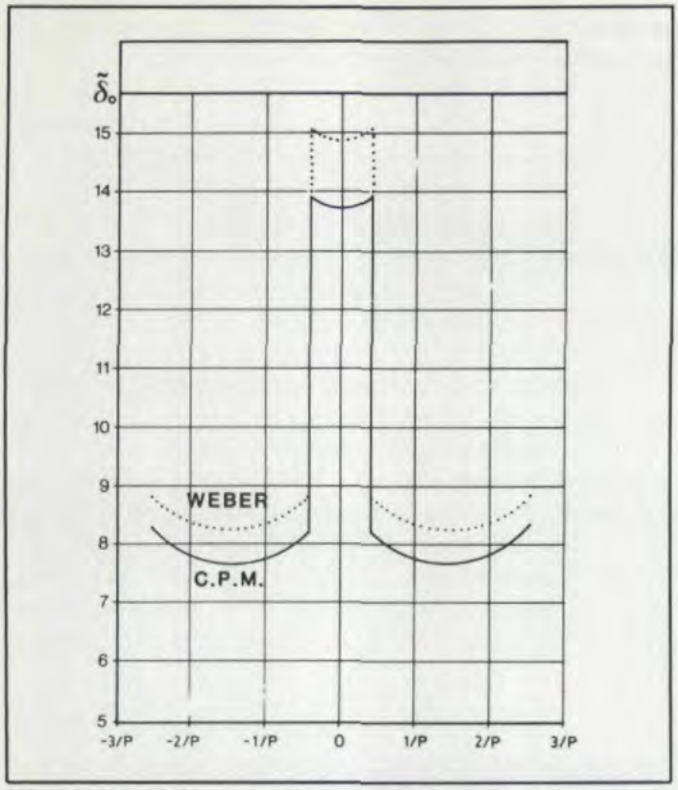

Fig. 9—Combined flexibility curve $\tilde{\delta}_0$ versus abscissa of load on line of action for a pair of identical standard AGMA gears (40 teeth, 20 deg); W = 1 000 lb/in., P = 0.5, comparison with Weber's curve.

of the contact zone as calculated from Hertz's theory. Contact width may be calculated at each point on the line of action and depends in a nonlinear fashion on absolute dimensions, material properties and transmitted load. This being known, the flexibility curve for the given pair of gears may be obtained, including the load sharing effect. Comparison with published results by Weber,[3] Chabert,[7] and Cornell[10] shows good agreement regarding the shape of flexibility curves, except for a slight shift between these curves, which is due, probably, to the selection of different reference points.

Acknowledgement: *Financial support from the National Sciences and Engineering Research Council of Canada is gratefully acknowledged. The authors wish also to thank Mr. A. Fortin for his help in numerical applications.*

This paper was presented at the Design Engineering Technical Conference, Cambridge, Mass., 1984 of the American Society of Mechanical Engineers. Paper No. 84-DET-85.

References

1. WALKER, M., "Gear Tooth Deflection and Profile Modifications: No. 1," *The Engineer,* Oct. 14, 1938, pp. 409-412.
2. WALKER, M., "Gear Tooth Deflection and Profile Modification: No. 2," *The Engineer,* Oct. 21, 1938, pp. 434-436.
3. WEBER, C., "The Deformation of Loaded Gears and the Effect on their Load-Carrying Capacity; Part I: Elastic Deformation of the Teeth and the Adjoining Parts of the Body of the Wheel," *Dept. of Scientific and Indus. Res.,* Sponsored Research (Germany), Report No. 3, (N. Report No. 102), 1949.
4. RICHARDSON, H. H., "Static and Dynamic Load, Stress and Deflection Cycles In Spur Gear Systems," *Ph.D. thesis,* M.I.T., Cambridge, MA, 1958.
5. WESTERGAARD, H.M., "Bearing Pressures and Cracks," ASME *Journal of Applied Mechanics,* Vol. 6, June 1939, pp. 49-53.
6. BARONET, C. N., and TORDION, G. V., "Exact Stress Distribution in Standard Gear Teeth and Geometry Factors," ASME *Journal of Engineering for Industry,* Vol. 95, No. 4, Nov. 1973, pp. 1159-1163.
7. CHABERT, G., DANG TRAN, T., and MATHIS, R., "An Evaluation of Stresses and Deflections of Spur Gear Teeth Under Strain," ASME *Journal of Engineering for Industry,* Vol. 96, No. 1, Feb. 1974, pp. 85-93.
8. PREMILHAT, A., TORDION, G. V., and BARONET, C. N., "An Improved Determination of the Elastic Compliance of a Spur Gear Tooth Acted on by a Concentrated Load," ASME *Journal of Engineering for Industry,* Vol. 96, No. 2, May 1974, pp. 382-384.
9. TOBE, T., KATO, M., INOUE, K., "True Stress and Stiffness of Spur Gear Tooth," *Proc. of the Fifth World Cong. on Th. of Mach. and Mech.,* Paris, 1979, pp. 1105-1108.
10. CORNELL, R. W., "Compliance and Stress Sensitivity of Spur Gear Teeth," ASME *Journal of Mechanical Design,* Vol. 103, No. 2, Apr. 1981, pp. 447-459.
11. CARDOU, A., and TORDION, G. V., "Numerical Implementation of Complex Potentials for Gear Tooth Stress Analysis," ASME *Journal of Mechanical Design,* Vol. 103, No. 2, Apr. 1981, pp. 460-465.

(continued on page 46)

Hob Length Effects

Y. Kotlyar
American Pfauter
Elk Grove Village, IL

Hobbing is probably the most popular gear manufacturing process. Its inherent accuracy and productivity makes it a logical choice for a wide range of sizes. Hobbing is successfully used for both roughing and finishing processes, depending on the accuracy required. Recent developments in cutting tool technology, such as coatings and improved materials, have proven hobbing processes to be even more competitive.

Optimum selection and utilization of cutting tools is essential for successful and economical gear hobbing. Hob material, feed and speed rates, gear material and hardness all influence hob performance. Hob length selection and its proper utilization can have a greater effect on performance than is usually realized.

Hob utilization would be ideal, if all hob cutting edges undergo an even cutting load, and consequently even wear. Unfortunately, in reality, only part of the hob is engaged in hobbing at a time, and even along this engagement zone cutting load is distributed unevenly. This causes some hob cutting edges to wear out more quickly than others. Hob shifting is used to offset this phenomenon. Hob wear distribution analysis helps to determine the benefit from utilizing the entire hob length, as well as the advantages from using longer hobs.

Cutting action divides hob length into four specific zones: non-usable, roughing, generating and shifting.

The non-usable zone is not suitable for metal removal, because the hob teeth in this area are not fully developed. This section is about one to one and a half pitches in length.

The roughing zone is the area where usually significant material removal occurs. Length of this zone is a function of gear-hob geometry, but depends primarily on the number of teeth on the gear. A relatively long roughing zone results in a more even distribution of cutting loads and creates a smoother cutting action. A very short roughing zone, occurring when hobbing gears with small numbers of teeth, creates excessive wear, due to the large amount of material removal per hob cutting edge. In this case, it is usually recommended to use a hob with a larger number of gashes.

The third region on the hob is designated the generating zone, as the involute is actually generated here. As such, it is critical that only sharp hob teeth operate in this area. The direction of shifting or movement of the hob, in relation to the workpiece, should be made so that the shift brings fresh hob teeth into the generating zone, and moves slightly worn teeth from the generating zone to the roughing zone. The generating zone represents the theoretical absolute minimum of hob length required to generate a gear. Locating this zone on the hob is essential for relative hob – workpiece positioning.

The remaining hob length, the "shifting zone", represents the amount of hob shift available. Availability of this zone makes it possible to offset the hob once part of it is worn out.

The so-called "engagement zone" is the sum of roughing and generating zones. The ratio between total hob length and length of engagement zone can be named "relative hob length". It is a more universal criteria to describe a real hob length value.

Fig. 1 shows wear distribution when the hob-workpiece relative position remains the same. Some of the hob cutting edges are worn out to the extent that further use may result in catastrophic breakage. Hob resharpening is necessary at this point, despite the fact that most of hob cutting edges are still suitable for hobbing.

If there is a provision for changing the hob-workpiece relative position (if hob length is greater than length of engagement zone) cutting load can be redistributed as some cutting edges wear out. Fig. 2 represents a wear pattern for longer hobs which are shifted at an optimum rate. Compar-

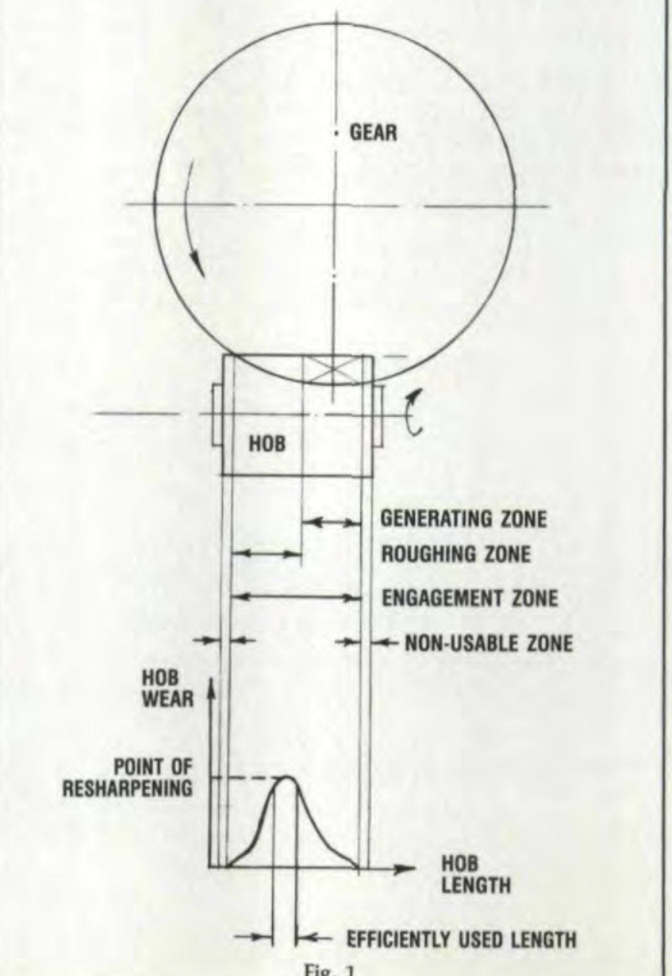

Fig. 1

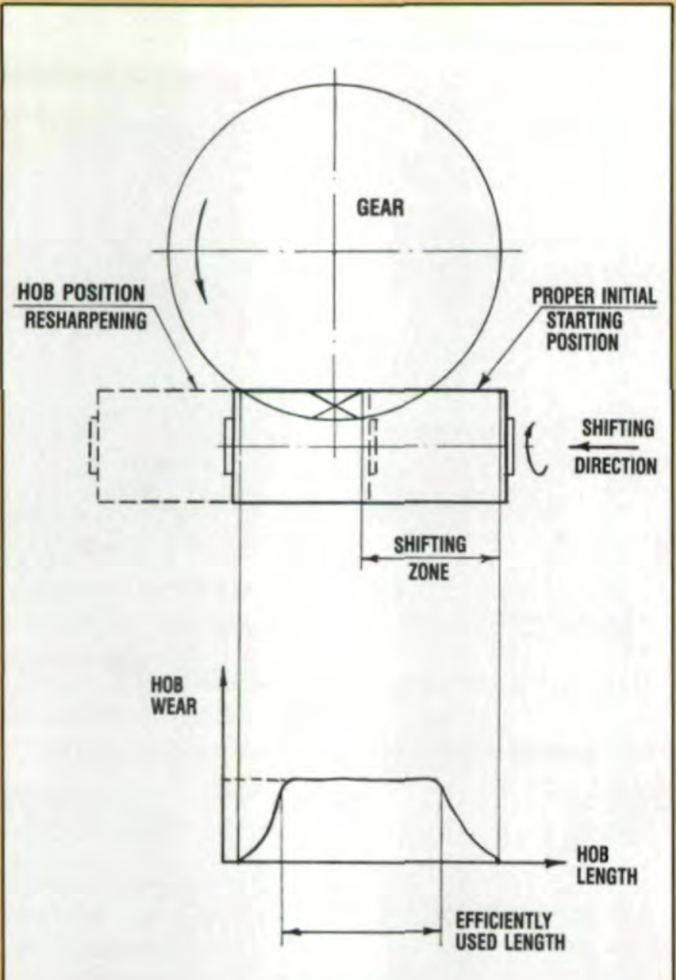

Fig. 2

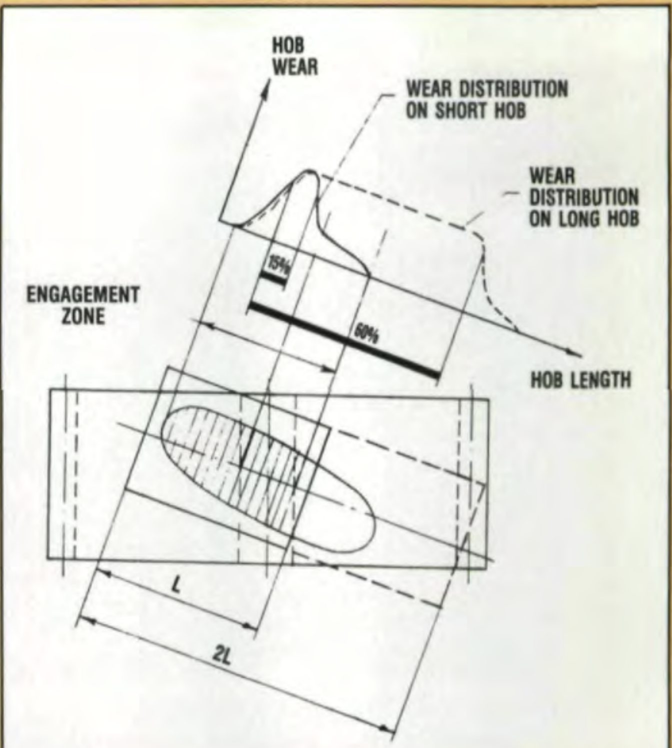

Fig. 3

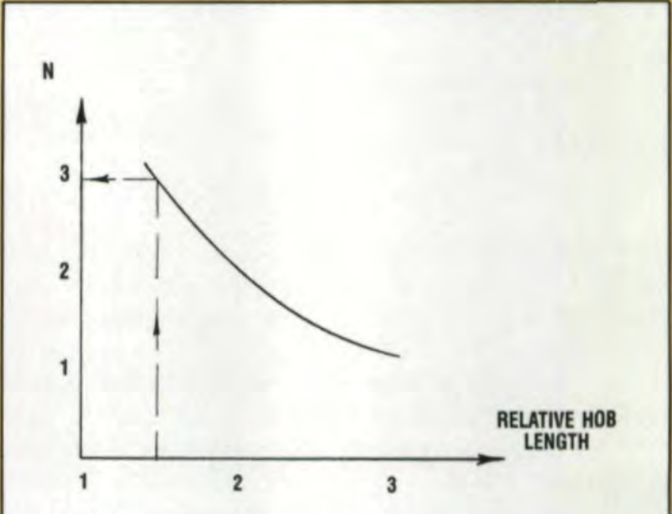

Fig. 4

ing Fig. 1 and Fig. 2, one can see that a greater percentage of hob length is being utilized in the latter case.

As an example, compare the performance of two hobs, one short and one long (Fig. 3). The length of the "short" hob is the sum of the engagement and non usable zones. The long hob is twice as long as the short hob. Reviewing the wear distribution charts, one can see that the short hob should be resharpened when approximately fifteen percent of the total hob length has been efficiently used. On the other hand, the long hob should be resharpened when approximately sixty percent of the total hob length is efficiently used.

Let's assume that the length of the short hob is equal to L, and the length of the long hob equals 2L. Then the efficiently used hob length is as follows:

small hob . . . . 15% × L
long hob . . . . 60% × 2L

The ratio of efficiently used long and short hob lengths or the actual gain from using the longer hob:

$$\frac{60\% \times 2L}{15\% \times L} = 8$$

This particular example indicates that 800% more gears can be cut by using a hob twice as long. Generally, the gain from using a longer hob can be calculated by:

Gain = [(length of longer hob) / (length of shorter hob)]^n

where n is obtained from Fig. 4 as a function of relative hob length. It can be noted that after the relative hob length exceeds a value of three, additional gain is almost proportional to hob length.

The above method can also be used to estimate the loss when the initial hob placement, in relation to the workpiece, is incorrect. For example, take the case of a hob, five inches in length, mispositioned by 0.5 inch, (a ten percent error). This gives the five inch long hob a working length of four and a half inches. Assuming that one and one half times the engagement zone of this hob is equal to 4.5 inches, in the above equation, n would be set equal to three (see Fig. 4). Plugging in the numbers, one can see that the loss from using a five inch long hob, with an effective length of four and

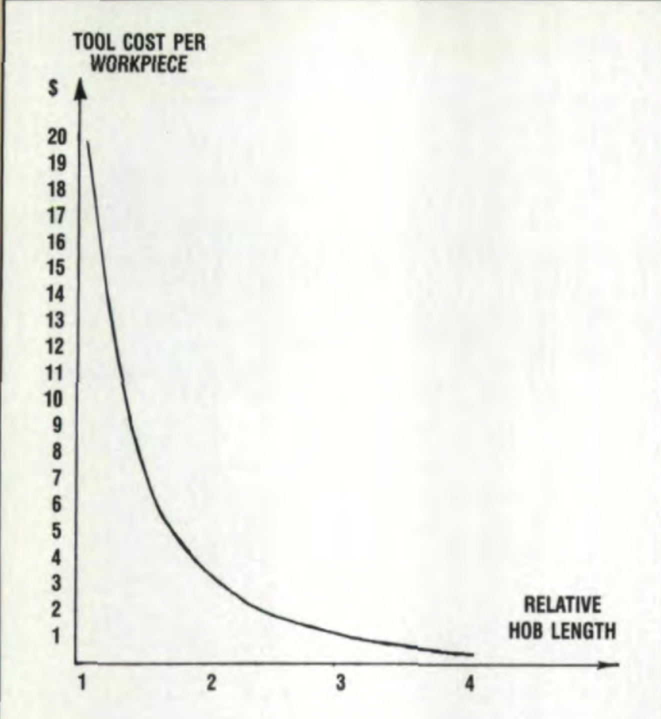

Fig. 5

a half inches, is 27.1%, almost three times as much as the initial error of 10%.

$$\text{Ratio} = \left(\frac{4.5}{5}\right)^3 = .729$$

$$\text{Loss} = (1 - 0.729) \times 100\% = 27.1\%$$

Fig. 5 shows the pattern of hob cost per workpiece as a function of relative hob length, considering that other cost influencing parameters remain the same. Cost figures are arbitrary and can be used only for comparison purposes.

Proper attention to hob length affects a substantial increase in hob life and time between resharpening. This leads to maximum tool and machine utilization, significantly reducing tool costs per workpiece while increasing productivity.

Obviously, close monitoring of hob wear distribution is necessary in order to benefit from the hob length effect. It is a rather easy task for mass production. For low quantity production, when the hob is frequently removed from the machine, it becomes a more difficult, but not impossible task, especially when utilizing hobbing machines with computerized controls.

APPENDIX

Method for calculating length of roughing, generating, and engagement zones:

1. GENERATING ZONE

Fig. 6 shows the generating zone in a transverse plane. The generating zone can be divided into two subzones:

A - length for generating dedendum

B - length for generating addendum

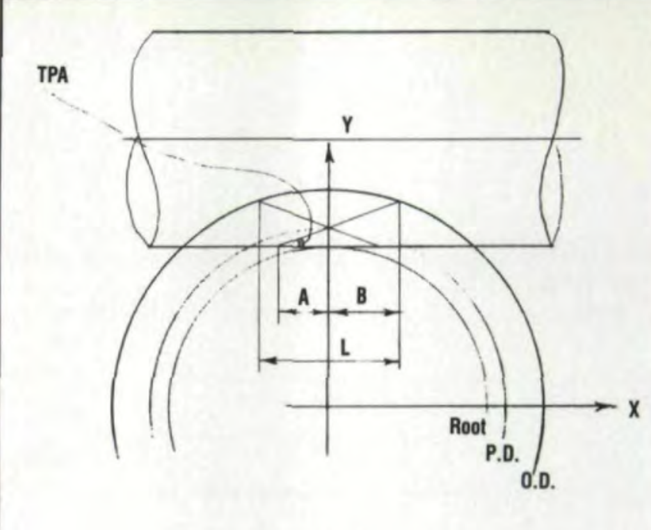

Fig. 6

It is important to know the value of both of these lengths. Then, by doubling the greater length, one can determine the total engagement zone in the transverse plane.

$$A = Ded/\tan(TPA)$$

where: Ded- gear dedendum

TPA- transverse pressure angle

The length "B" can be determined as an X-coordinate of the intersection of the workpiece's outside diameter with the action line by utilizing formulas for a circle and a straight line.

The equation for the outside diameter of the workpiece:

$$X^2 + Y^2 = (WD/2)^2$$

where: WD- outside diameter of workpiece

The equation of the line of action:

$$Y = PD/2 + X \times \tan(TPA)$$

where: PD- pitch diameter of the workpiece

By solving this system of two equations, one determines the coordinates of the two intersections of the line of action with the outside diameter of the gear. Only one of the two intersections is to be considered.

$$B = X = \frac{-b + \sqrt{b^2 - 4 \times a \times c}}{2 \times a}$$

where: $a = 1 + \tan^2(TPA)$

$b = PD \times \tan(TPA)$

$c = (PD/2)^2 - (WD/2)^2$

Thus, the total generating length "L" in the transverse plane *is as follows:*

$L = 2 \times A$ if $A>B$

$L = 2 \times B$ if $B>A$

To determine the actual hob generating zone, one can project the length "L" onto the axis of hob rotation:

Generating zone: $Lg = L/\cos(q)$

where: q - swivel angle of the hob

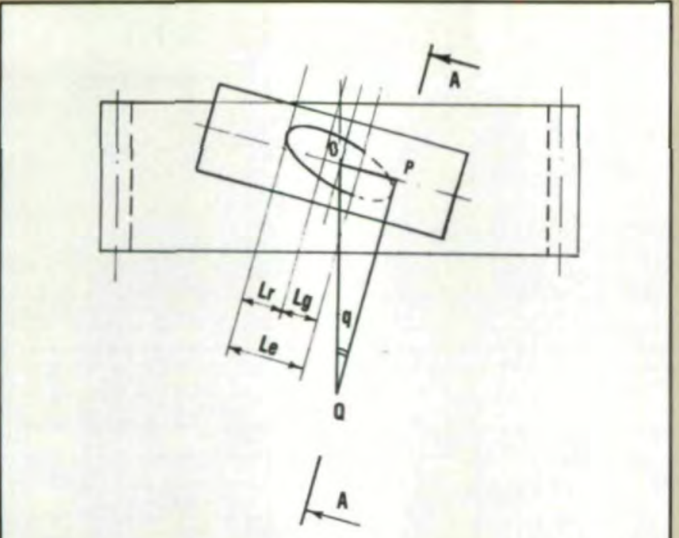

Fig. 7

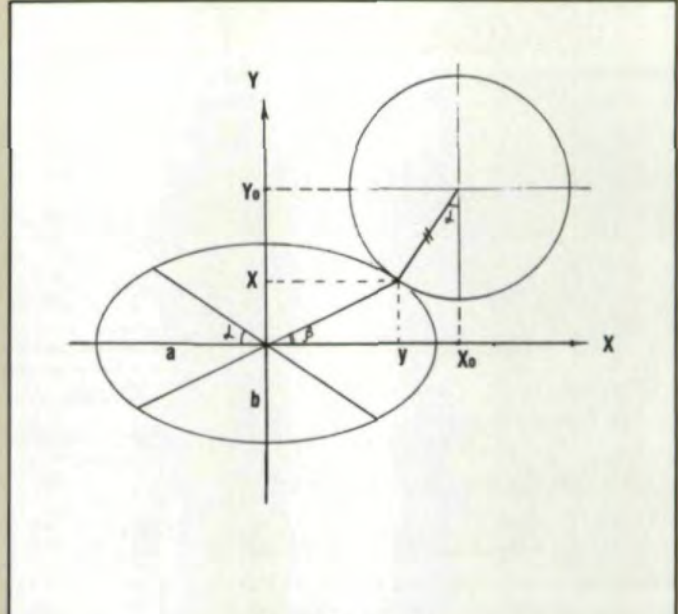

Fig. 8 View A-A

2. ROUGHING ZONE

The method shown below for determination of the roughing zone is valid for both spur and helical gears. The intersection of the O.D. of the hob with the O.D. of the workpiece is a 3-dimensional curve. The curve projection on a plane is an ellipse.

On Fig. 7 one can see that the distance from the pivot point to the start of roughing zone can be found from the triangle OPQ:

$$OP = QP \times \tan(q)$$

where QP can be determined by considering cross section AA perpendicular to the center line of the hob and tangent to the ellipse mentioned above.

This intersection is shown on Fig. 8, where the ellipse is the cross section of the gear, and the circle is the cross section of the hob. Placing a coordinate system at the ellipse center allows writing equations of the circle, the ellipse, and the line passes through the circle center and the common point of the circle and the ellipse.

2.1 Hob circle: $$(X-Xo)^2 + (Y-Yo)^2 = (HD/2)^2$$

where: HD- hob outside diameter
Xo- coordinate of the circle center
$Yo = WD/2 + HD/2 - wd$ coordinate of the circle center

where: wd- whole depth of the tooth

2.2 Workpiece ellipse: $$(X/a)^2 + (Y/b)^2 = 1$$

where: $a = WD/2 \times \sin(q)$ major radius of the ellipse
$b = WD/2$ minor radius of the ellipse

2.3 Line: $$(Y-Yo) = (X-Xo)/\tan(\delta)$$

From the characteristics of an ellipse, $\tan(\delta)$ can be obtained as a function of known values:

$$\tan(\delta) \times \tan(\beta) = (b/a)^2$$
$$\tan(\beta) = Y/X$$

so $$\tan(\delta) = (b/a)^2 \times (X/Y)$$

Consequently the equation 2.3 can be rewritten as follows:

2.3 Line: $$(Y-Yo) = (X-Xo)/(\,(b/a)^2 \times (X/Y)\,)$$

To solve this system of three equations with three unknowns (X, Y, Xo), one can isolate Y and get an equation of the 4th degree as follows:

$$KA \times Y^4 + KB \times Y^3 + KC \times Y^2 + KD \times Y + KE = 0$$

where: $KA = (dr \times a)^2 - b^2$
$dr = \sin^2(q)$
$KB = (2 \times Yo \times b^2) - (2 \times Yo \times a^2 \times dr^2)$
$KC = (b \times rh)^2 - (Yo \times b)^2 + (Yo \times dr \times a)^2 - (dr \times a \times b)^2$
$rh = HD/2$
$KD = 2 \times Yo \times (dr \times a \times b)^2$
$KE = (-1)(Yo \times dr \times a \times b)^2$

This equation can be solved by Newton's approximation method, where each next iteration value is calculated by the formula:

$$Yn = Y_{n-1} - F(Y_{n-1})/F'(Y_{n-1})$$

where: $F(Y) = KA \times Y^4 + KB \times Y^3 + KC \times Y^2 + KD \times Y + KE$
F'(Y) is first derivative of the function F(Y)

(continued on page 48)

Single Flank Data Analysis and Interpretation

Robert E. Smith
Gleason Works
Rochester, New York

Introduction

Much of the information in this article has been extracted from an AGMA Technical Paper, "What Single Flank Testing Can Do For You", presented in 1984 by the author.[1]

Single flank gear testing is a subject of increasing interest. Although it has been widely used and understood in Europe, its use has remained relatively rare in this country. However, as the measuring devices become smaller, less expensive and have better accuracy and resolution, they become more attractive as a production measuring device.

Single flank testing is concerned with the measurement of a parameter called Transmission error. Transmission error is defined as the deviation of the position of the driven gear, for a given angular position of the driving gear, from the position that the driven gear would occupy if the gears were geometrically perfect.[2]

Transmission error is generally seen in the form of a fairly regular once per tooth pattern, superimposed on large waves related to once per revolution type errors. Noise and vibration excitation is generally related to the once per tooth pattern, while accuracy problems are more generally related to the once per revolution type patterns.

It will be shown later that the study of noise excitation is more closely related to profile shape and the involute tooth form. Gear elements with perfect, rigid, uniformly spaced involute teeth transmit exactly uniform angular velocities.[3]

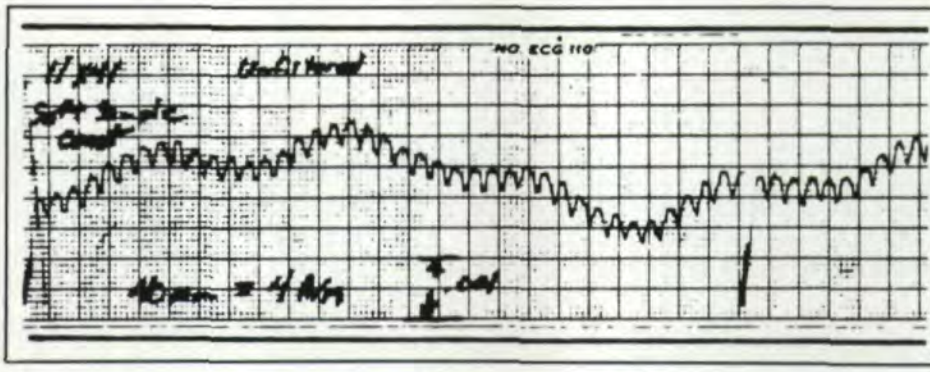

Fig. 1

Measuring Device

A description of the measuring device, based on optical encoders, will be found in reference[1] and.[4] The encoders and associated electronics generate an analog signal that is directly related to portions of involute or profile variations, pitch variation, runout, and accumulated pitch variation. The graph in Fig. 1 illustrates a recording of a typical 11 × 41 pair of gears. The data shows two revolutions of the ring gear. The relationship of these parameters of gear geometry to the generated waveform is also described in the above two references.

Interpretation of Data

ANALOG DATA: The recording in Fig. 2 represents one revolution of a typical gear, run with a perfect master. Many bits of information can be read from this graph. These are: burr amplitude, adjacent pitch variation (f_p), accumulated pitch variation (F_p), tooth to tooth composite-single flank, (f_i'), total composite-single flank (F_i), and effective profile or conjugacy. If two non-miter test gears are run together, it is also possible to evaluate accumulated pitch variation for each gear separately, but the effective profile or conjugacy is the result of the combined tooth shapes of the two gears. If the gears are miters, it is possible to phase the accumulated pitch variation of each so that the resulting error is minimized.

Fig. 3 shows the resulting bar graph from a single probe/precision index test superimposed on a single flank test, of the same gear, run against a perfect master gear.

Examining the analog graph of a single flank test is always the best place to start with data analysis. The unfiltered, total information presents a good visual picture of the overall gear quality. Most instruments have provisions for use of high and low pass filters that aid in the separation and analysis of tooth to tooth type errors from runout type errors. Also, viewing analog curves of profile errors is useful in the determination of corrective actions (See Fig. 4).

REAL TIME ANALYSIS: Many times, the analog data becomes too complex to analyze in that form. This is due to various causes: running two test gears together, burrs, amplitude or frequency

AUTHOR:

ROBERT SMITH, *Senior Manufacturing Technology Engineer at Gleason Machine Division, has over thirty years experience in the Gear Industry. Mr. Smith received his training from Rochester Institute of Technology. While at Gleason, Mr. Smith's engineering assignments have included gear methods, manufacturing, research and gear quality. These assignments involved the use and application of instrumentation for the study of noise, vibration, and structural dynamics. From these assignments, he expanded his ideas relating to gear metrology. Currently, Mr. Smith is chairman of the Measuring Methods and Practices and Master Gear Subcommittee in the American Gear Manufacturers Association, and is also a member of the Rochester Industrial Engineering Society and Society of Experimental Stress Analysis.*

Arrow Gear uses the latest in CNC grinding technology.

You can too!

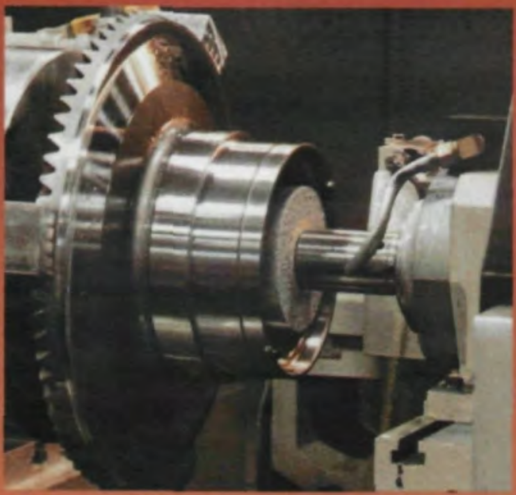

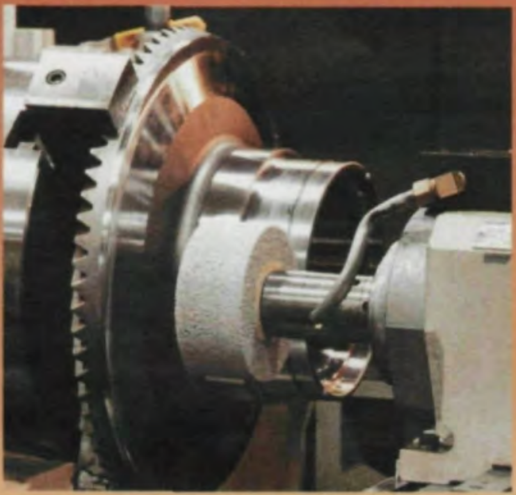

A leading gear manufacturer grinds 11 surfaces in one operation on their new Bryant Lectraline® CNC grinder.

Mr. Joseph Arvin, Executive Vice President and General Manager of Arrow Gear Company, Downers Grove, Illinois, sent his salesmen a memo. It read: "What happens when you put Arrow Gear skill and experience together with the latest in CNC grinding technology . . . UNPARALLELED QUALITY, FASTER DELIVERY, AND COST SAVINGS.

"This bevel gear operation on the Jeff 'B' LCAC Landing Craft has 11 OD's, ID's, and faces ground in one chucking on our Bryant LL3-55 CNC Grinder.

"Combining what would be a tedious, three machine, six operation finish grind into a straight-forward one operation grind means quality, on time delivery, and cost savings to our customer."

Mr. Arvin liked the first Bryant so well that he ordered another. *NEED WE SAY MORE?*

Interested in what a Bryant Lectraline can do for your grinding operations? Contact us. Bryant Grinder Corporation, Springfield, VT 05156, (802) 885-5161. We'll tell you.

In a hurry? Call our 24 hour, toll-free hotline, 1-800-453-2100, Ext. B215.

Bryant®

BRYANT GRINDER CORPORATION
a subsidiary of
Ex-Cell-O Corporation

CIRCLE A-8 ON READER REPLY CARD

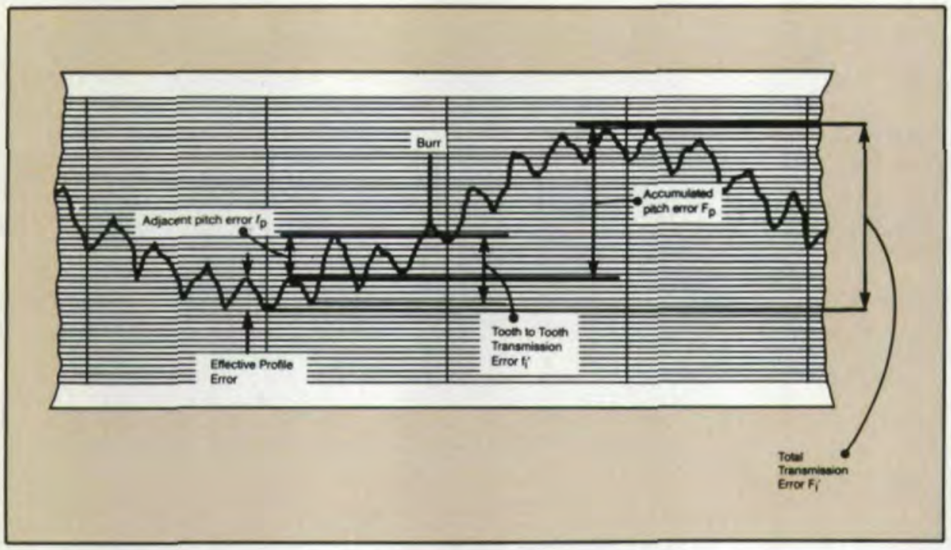

Fig. 2

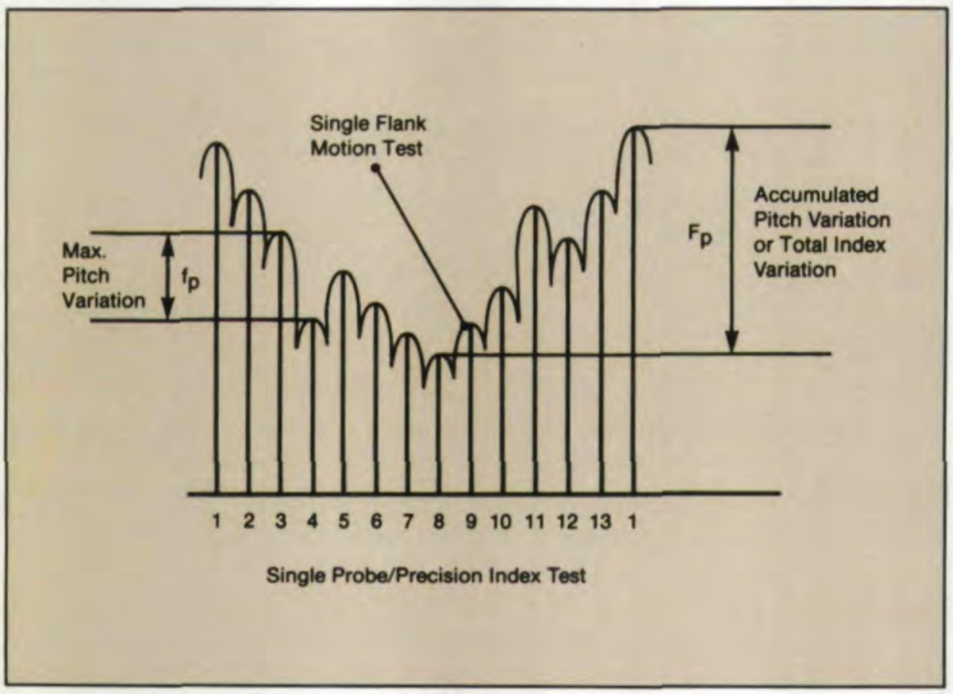

Fig. 3

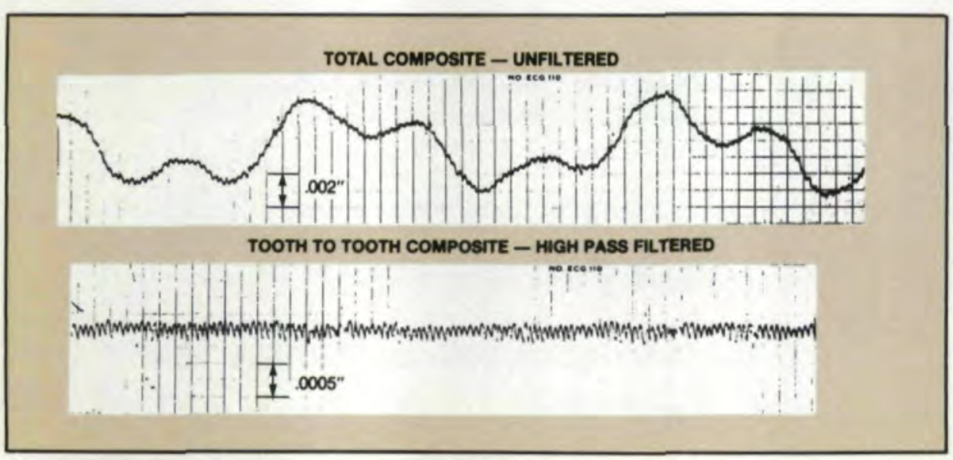

Fig. 4A

modulation, runout of gear and pinion phasing in and out, flats on tooth surface, etc. In these cases, it is useful to use a real time analyzer which performs a fast Fourier transform on the data. This converts the information from the time domain to the frequency domain.

Fig. 4b shows frequency domain data for the same gears. By taking several averages of the sampled data, it is possible to read repeatable amplitude values of the various frequencies contained in the analog chart. Mark[3] breaks this spectral data into two components. The "mean" geometric deviation component for a gear or pinion is defined, as the tooth surface formed, by taking the average of all tooth surfaces on the pinion or gear under consideration. The "random" component of the geometric deviation of a tooth surface is defined as the deviation of that tooth surface from the mean. The mean component comes from intentional or accidental profile modifications, while the random component comes from the runout effects. The mean component of the geometric deviations gives rise to the tooth meshing harmonics of vibratory excitation. Whereas, the random component of the geometric deviations gives rise to the rotational harmonics, and especially, to the sideband components of the spectrum which occur at the tooth meshing harmonic frequencies, plus or minus one or a few rotational harmonic frequencies.

TIME HISTORY AVERAGING: The use of time averaging, in the time domain, is a technique that has seen little use, so far, in single flank testing. However, in the future, it should become very common. It requires the use of an accurate once per revolution marker pulse on each shaft. Data from many revolutions of a given shaft are averaged together and, therefore, information that is synchronous with the marker will remain, while non-synchronous data will eventually average to zero. The advantage of this technique is that it allows one to separate out elemental errors, such as once per tooth conjugacy, pitch variation, and accumulated pitch variation attributable to each individual gear. In Fig. 5, Smith[5] shows the time history data of a twin mesh gearbox, as well as time averaged data of the individual gears in the same box. Time history averaging offers some very interesting possibilities.

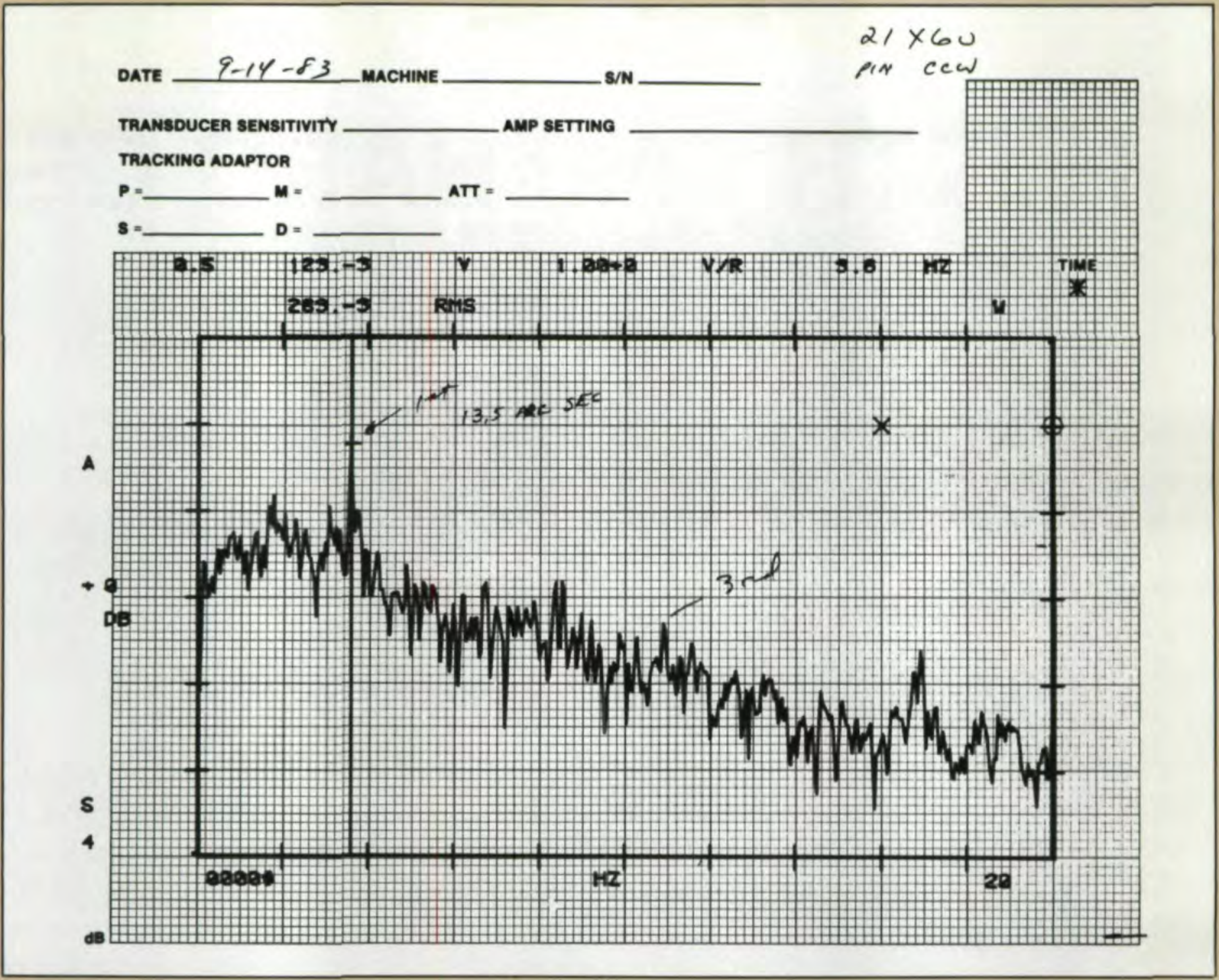

DATE 9-14-83 MACHINE S/N
21 X 60
PIN CCW
TRANSDUCER SENSITIVITY AMP SETTING
TRACKING ADAPTOR
P = M = ATT =
S = D =
1st 13.5 ARC SEC
3rd
A
DB
S
4
dB
HZ
20
TIME

Fig. 4B

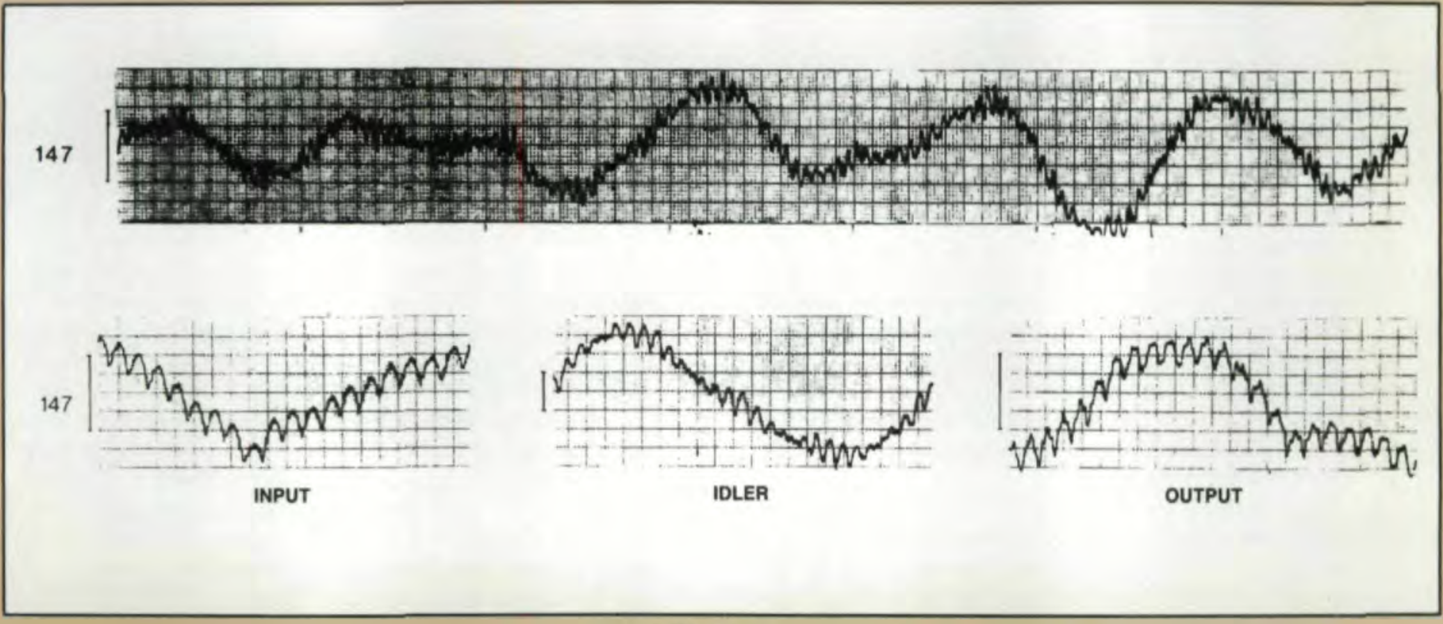

147
147
INPUT
IDLER
OUTPUT

Fig. 5

The State of the Art...

HURTH CNC HARD GEA

The HURTH hard finishing process is an entirely new approach to gear manufacture and finishing because it enables the manufacturer to alter the geometry of the teeth while smoothing the tooth flank surfaces of external and internal hardened gears. This process can correct errors in profile, spacing and lead, as well as such parameters as radial runout, pitch and cumulative pitch. The end product is a more accurate, smoother, quieter-running gear.

To accomplish this, the tool flank and the work gear flank being machined are positively guided in such a way that the workpiece and tool are rigidly linked during machining with the tool performing a plunge-feed motion for stock removal. All right-hand flanks are finished first. The machine then reverses and finishes left-hand flanks. This single-flank contact means no broken-out tool teeth due to workpiece defects and permits correction or "redesign" of the workpiece gear during finishing.

The tool, either Borazon® or ceramic, is conditioned and profiled for the work gear geometry and desired stock removal by using a coated dressing master. Dressing takes no longer than the time required to finish one workpiece and each dressing removes a minimal amount of material from the tool surfaces.

R FINISHING MACHINES

The hard finishing process gives the widest range of applications of all post-hardening gear finishing methods. Adjacent shoulders or collars rarely pose serious problems.

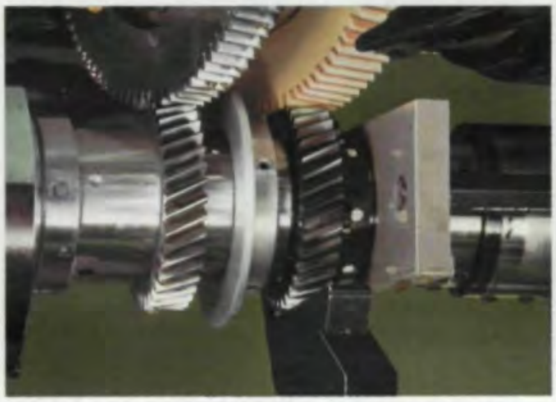

This illustration shows the tool finishing the work-piece gear and the external master gears engaged to control the operation.

Other advantages of the process:

- AGMA Class 14 achievable.
- Definitely no grinding burns.
- Tool marks run diagonally to gear diameter.
- Permits machining of gear teeth adjacent to shoulders.
- Equipment is ideal for automated work handling.

Please write or phone for details on this revolutionary new process.

STARCUT SUPPLIED PRODUCTS FOR PRODUCTIVITY

Star Machine Tools

Standard and CNC Hob Sharpeners
Shaper Cutter Sharpeners
CNC Drill and Reamer Sharpeners
Keyseaters

Star Cutting Tools

Hobs
Form-Relieved Cutters
Gun Drills
Gun Reamers
Keyseat Cutters

Gold Star Coatings

Hurth Machine Tools

Standard & Automatic Keyway and Slot Milling Machines
Automatic Spline Shaft Milling Machines
CNC Gear Hobbing Machines
CNC Gear Shaving Machings
Shaving Cutter Grinding Machines
Gear Testing Machines
CNC Gear Tooth Chamfering Machines
Gear Deburring Machines
CNC Hard Gear Finishing Machines

Stieber Precision Clamping Tools

Planring Flexible Machining Systems

Star Since 1927

STARCUT SALES, INC.
23461 Industrial Park Drive
Farmington Hills, MI 48024
313/474-8200 Telex 230-411

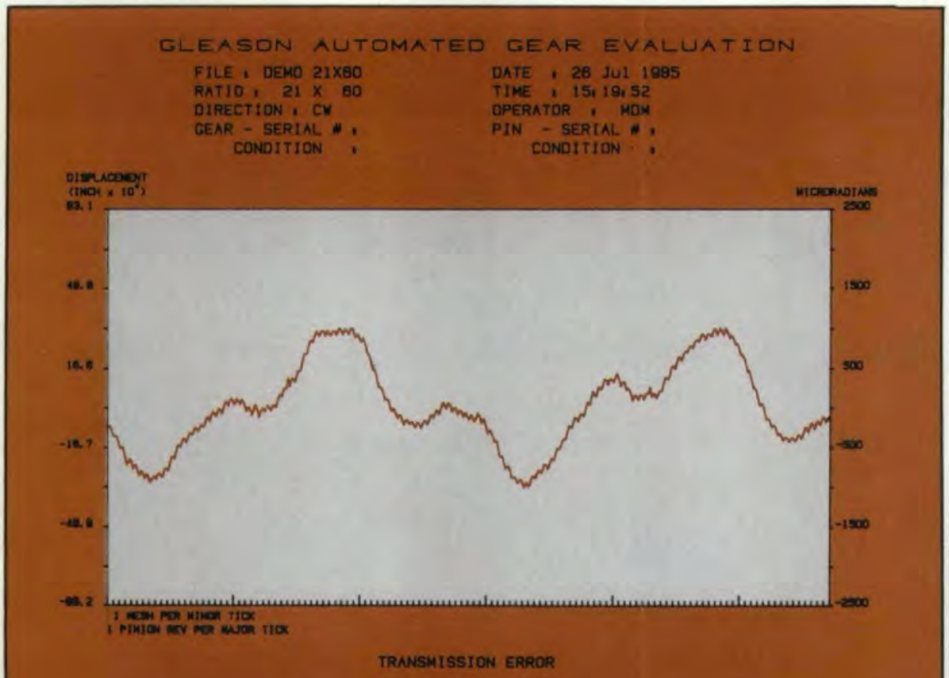

Fig. 6A

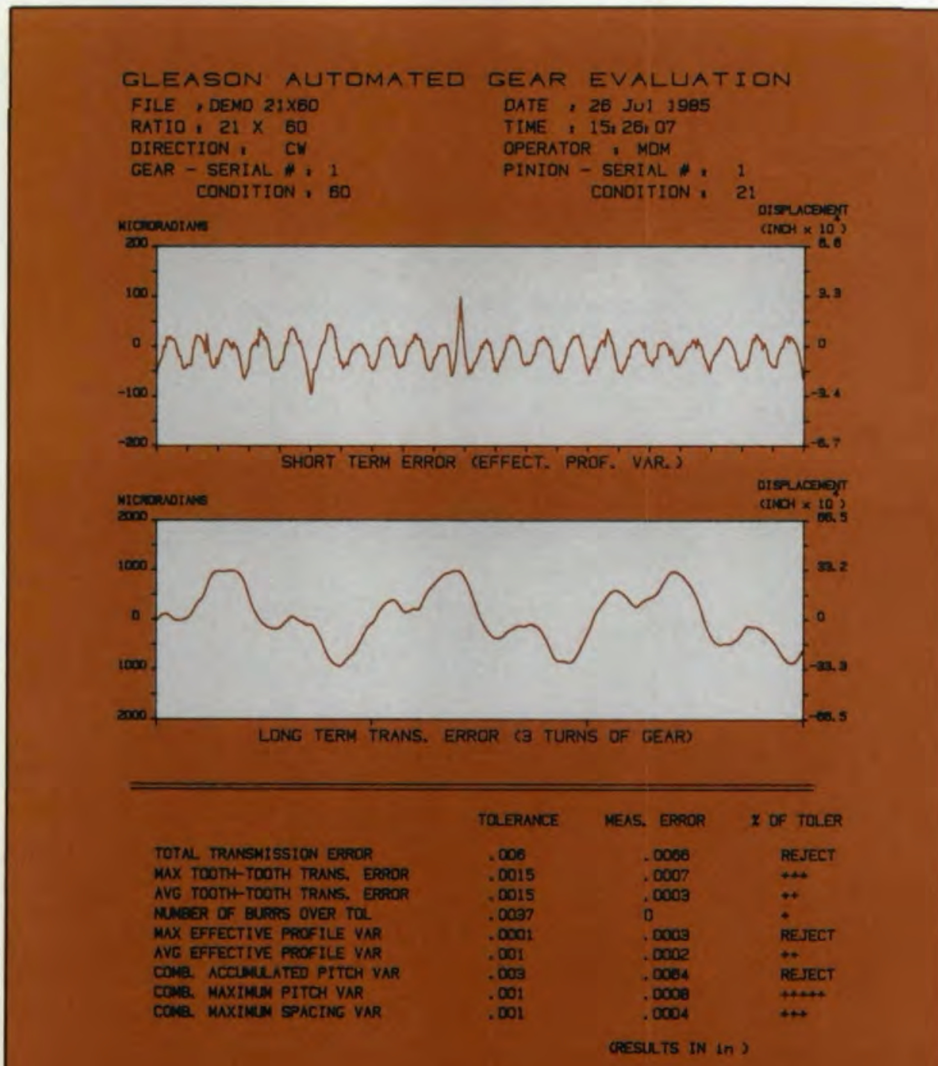

Fig. 6B

AUTOMATIC DATA ANALYSIS (COMPUTERIZED): In order to minimize the need for a skilled engineer or technician to analyze data, computers and appropriate software packages are now available for single flank testers. The computers are programmed to extract quantitative information, related to the various measureable parameters, from the complex analog data. These values can then be compared to previously established tolerance limits. The accept/reject judgements can be made by computer.

Visual data can also be displayed in forms unavailable in the other methods of data analysis described above. A typical series of displays would include the following:

1. Total transmission error
2. Long term component (related to once/rev. type errors)
3. Short term component (related to once/tooth type errors)
4. Average effective profile error (average component described in reference)[3]
5. Velocity and acceleration derivatives of 4 above (to look at the effect of peak acceleration caused by displacement waveshape)
6. FFT spectral analysis of data (also includes velocity and acceleration displays).

There are many other uses of computerized data analysis, such as master gear error correction, pitch variation, accumulated pitch variation, runout, comparison to AGMA, DIN, ISO, or company standards as well as statistical quality control and statistical process control. Fig. 6-6F shows some of this data.

Advantages of Single Flank Over Double Flank Testing

APPARENT PROFILE ERRORS: Munro[2] shows how profile errors affect the motion curves of a gear running with a master (Fig. 7). Curves of various tooth shapes are shown for single and double flank tests.

Double flank testing is a fast, inexpensive way to composite test gears, but it is usually impossible to interpret the tooth to tooth data in terms of elemental or transmission error. This is due to both sets of flanks being in mesh at one time.

Single flank composite testing does measure transmission error directly. Because the gears run with only one set of flanks in mesh (with backlash) it is possible to interpret the curve in terms of profile and pitch errors.

Munro concludes:

1. The single flank test always shows the profile error of the flank in mesh, but not over the whole of the flank.
2. The dual flank test gives a composite curve of the two flanks, and there is no method of ascribing an error to a particular flank.
3. The dual flank peak to peak value (tooth to tooth composite error) is often, but not always, approximately equal to the single flank peak to peak value multiplied by half the cotangent of the pressure angle.
4. With a barrelled profile error, the dual flank test gives a waveform with two peaks per tooth pitch.
5. The dual flank curve is sometimes identical for two quite different sets of profile errors.

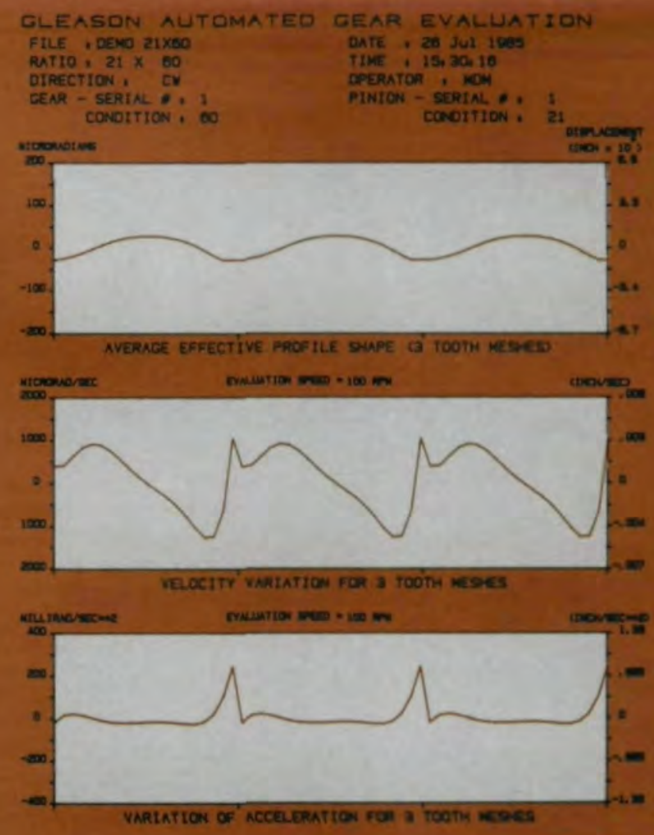

Fig. 6C

RUNOUT VS. ACCUMULATED PITCH VARIATION: The ability to check accumulated pitch variation is an important attribute of single flank testing. First of all, there is a difference between "runout" and "accumulated pitch variation." A gear with runout does have accumulated pitch variation. A gear with accumulated pitch variation does not necessarily have runout.

Runout occurs in a gear with a bore or locating surface that is eccentric from the pitch circle of the teeth. Runout is shown as a variation in depth of a ball type probe as it engages each successive tooth slot. Or, it can be a large total composite variation, if it is observed on a single flank tester.

A gear can be produced, by various means, that will have little or no runout, as described above, and it will show excellent results when tested with a ball check or by a double flank test. This happens when a gear is cut with runout and then shaved or ground on a machine that does not have a rigid drive coupling the tool to the workpiece.

When the gear is cut with an eccentric pitch circle, the slots are at different radii and angular positions. When the gear is

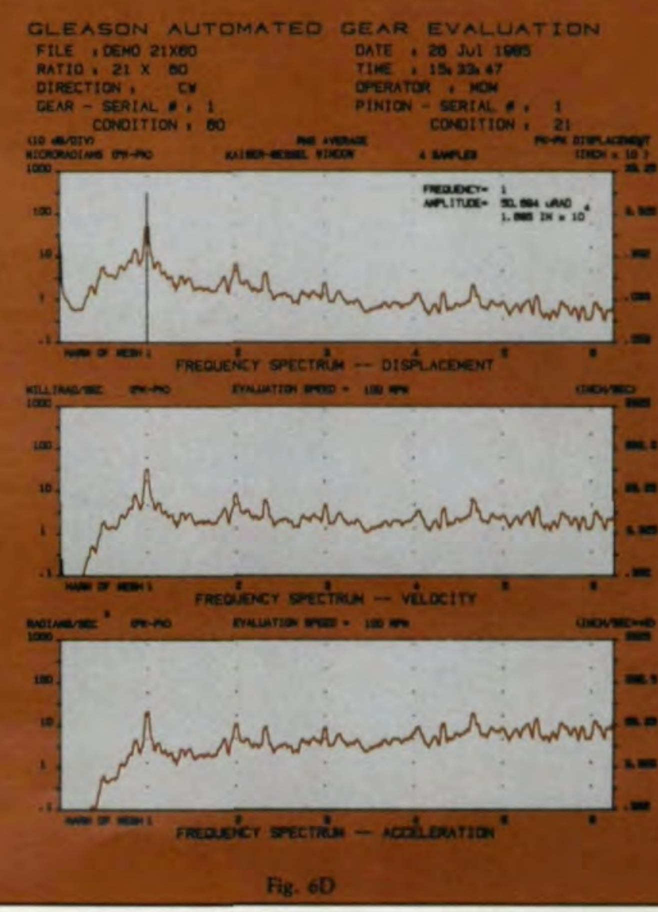

Fig. 6D

GLEASON AUTOMATED GEAR EVALUATION

FILE : DEMO 21X60	DATE : 26 Jul 1985
RATIO : 21 X 60	TIME : 15:44:35
DIRECTION : CW	OPERATOR : MDM
GEAR - SERIAL # : 1	PINION - SERIAL # : 1
CONDITION : 60	CONDITION : 21

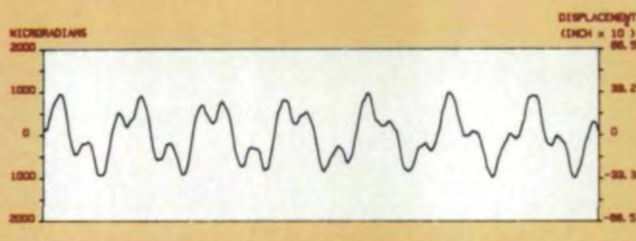

LONG TERM TRANSMISSION ERROR

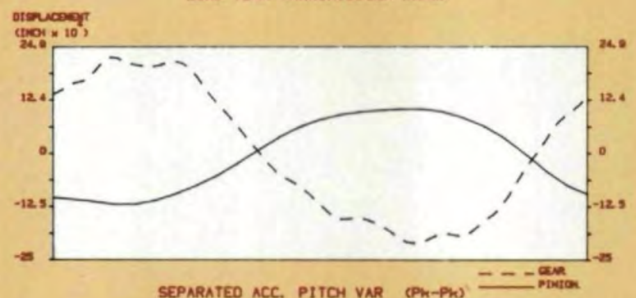

SEPARATED ACC. PITCH VAR (Pk-Pk)

	TOLERANCE	MEAS. ERROR	% OF TOLER
PINION ACC. PITCH VAR :	.003	.00225	****
GEAR ACC. PITCH VAR :	.004	.00436	REJECT

Fig. 6E

GLEASON AUTOMATED GEAR EVALUATION

FILE : DEMO 21X60	DATE : 26 Jul 1985
RATIO : 21 X 60	TIME : 15:46:32
DIRECTION : CW	OPERATOR : MDM
GEAR - SERIAL # : 1	PINION - SERIAL # : 1
CONDITION : 60	CONDITION : 21

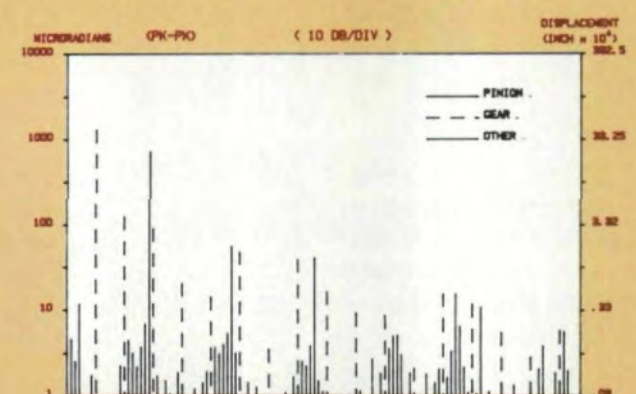

HARMONICS OF ROTATION

	PINION			GEAR		
HARMONIC	TOLERANCE	MEASURED	% OF TOL	TOLERANCE	MEASURED	% OF TOL
1	0	.002347		0	.004316	
2	0	.000183		0	.000413	
3	0	.000135		0	.000298	
4	0	1.8E-5		0	6.8E-5	
5	0	3.5E-5		0	4.7E-5	
6	0	1.8E-5		0	.000159	
TOTAL ACC. PITCH VAR	.003	.002256		.004	.004383	

Fig. 6F

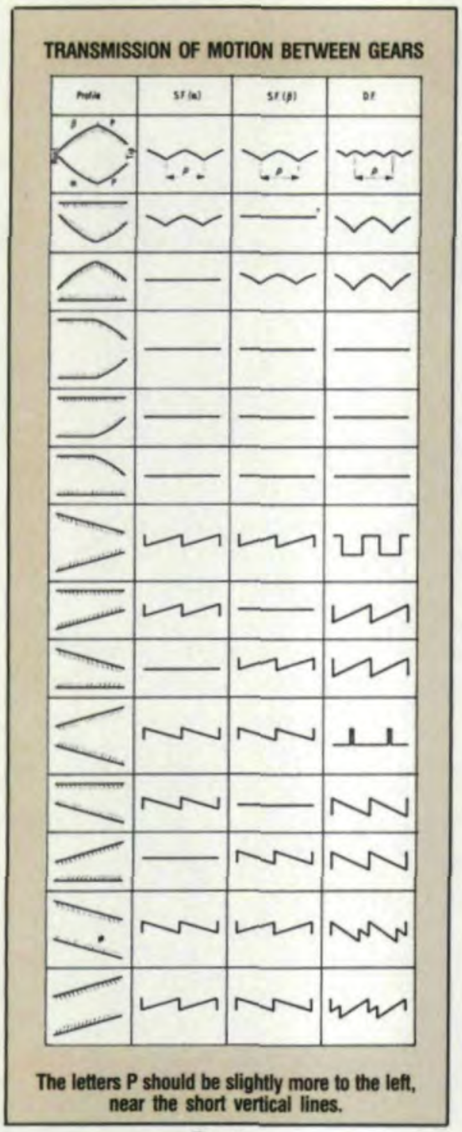

Fig. 7

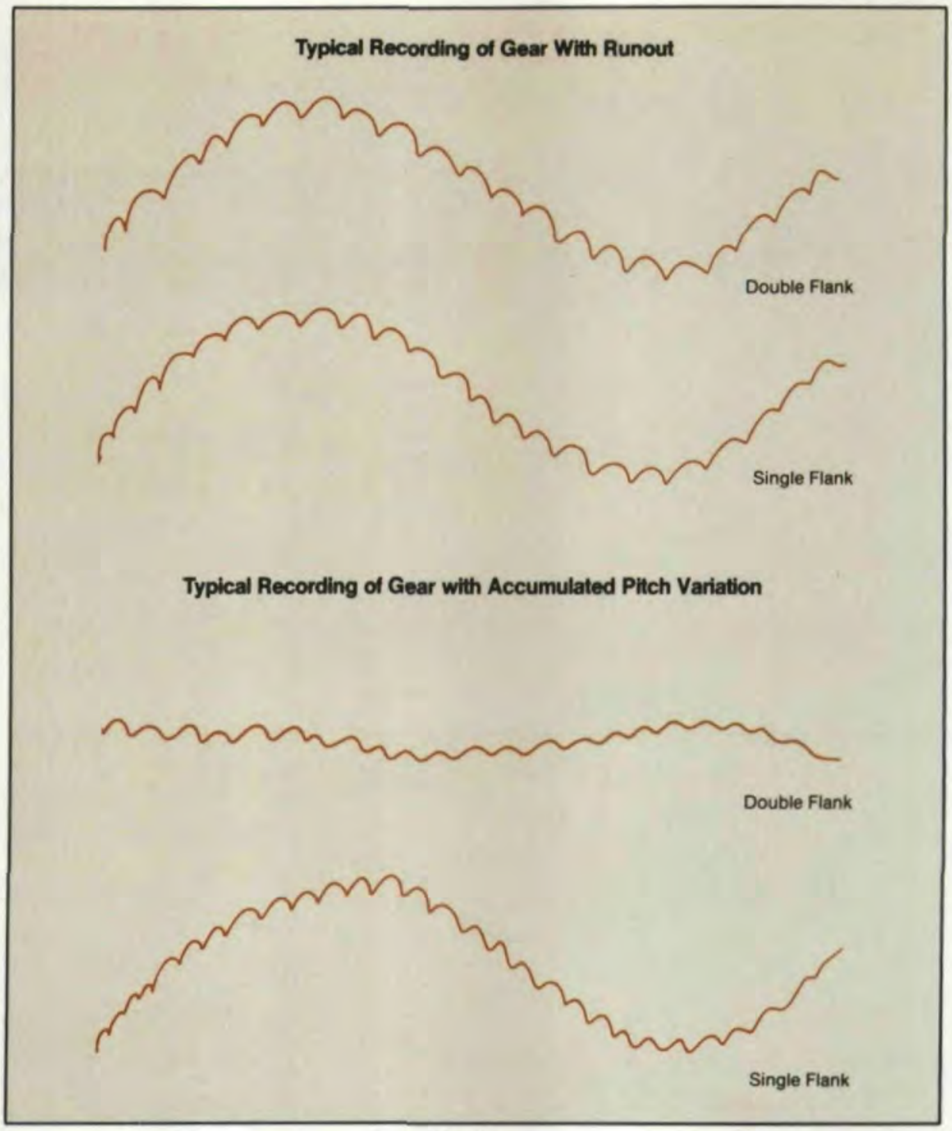

Fig. 8

shaved, it is run with a tool that maintains a constant rigid center distance, but is not connected to the workpiece by a drive train. The tool also cuts an equal amount of stock from each flank of every tooth. Therefore, all slots are now machined to the same radius, from the center of rotation, and are displaced from *true angular position* by varying small amounts. The resulting gear has very small amounts of individual pitch variations, but has a large accumulated pitch variations, to which the single flank tester responds.

These accumulated pitch variations have all the undesirable effects of a gear with traditional runout. It would check "good" by either a ball check or a double flank composite test. Fig. 8 illustrates the advantage of single flank for the two situations.

Application of Data

Before using the single flank data in an application, it is first necessary to define the problem. There are three basic areas of concern: noise, accuracy, and strength or durability. In a general way, single flank data in the form of tooth to tooth transmission error is related to noise and vibration; total transmission error is related to accuracy, and both types relate to strength in a secondary way. Lead is the element primarily associated with strength and this is best measured, by other means, such as contact patterns. Fig. 9 is a very generalized chart of cause and effect relationships. When evaluating noise problems, it is appropriate to run a sound analysis test with a real time analyzer to pinpoint the offending rotational order. In most cases, it will be at tooth mesh frequencies, however, when running at very high RPM, it will be at the once per rev. frequency.

When it comes to accuracy, all types of transmission errors will have an effect. Accumulated pitch variation will normally be the greatest contributor to total transmission error and inaccuracy.

Case Histories

The following case histories are included to demonstrate the capabilities of single flank testing.

(1) NOISE: Fig. 10 is used to illustrate the fact that accuracy isn't necesary for noise control. It shows a lapped hypoid pair of gears with a relatively large total transmission error from accumulated pitch and bolt hole distortions, but with a very low tooth to tooth transmission error (less than .0001"). This was a quiet pair in the axle.

Application of Single Flank Data

DEFINE PROBLEM!

Problem	Primary Application	Cause
Noise	Vehicle - High Frequency >100 Hz	Effective Profile
	Vehicle - Low Frequency <100 Hz	Accumulated Pitch Variation
	Machine Tools - High Frequency	Effective Profile
	Power Transmission - High Frequency > 100 Hz	Effective Profile
	Power Transmission - Low Frequency < 100 Hz	Accumulated Pitch Variation
	Aircraft Drives High RPM - (30,000)	Accumulated Pitch Variation
Problem	**Primary Application**	**Cause**
Positional Accuracy	Machine tools, indexing devices, Gun directors, robots, etc.	S.F. T.T. Composite S.F. Total Composite Pitch Variation Accumulated Pitch Variation
	Secondary Application	
Strength - Fatique	Marine & Power Drives	Use contact pattern or lead measurements for primary control S.F. profile, pitch variation, & accumulated pitch variation for secondary control

The above are generalities.

There will be exceptions such as:
- Sidebands (Sum and Difference Frequencies)
- Contact Ratio — Helicals
  - — Spirals
  - — Lead Error

Fig. 9

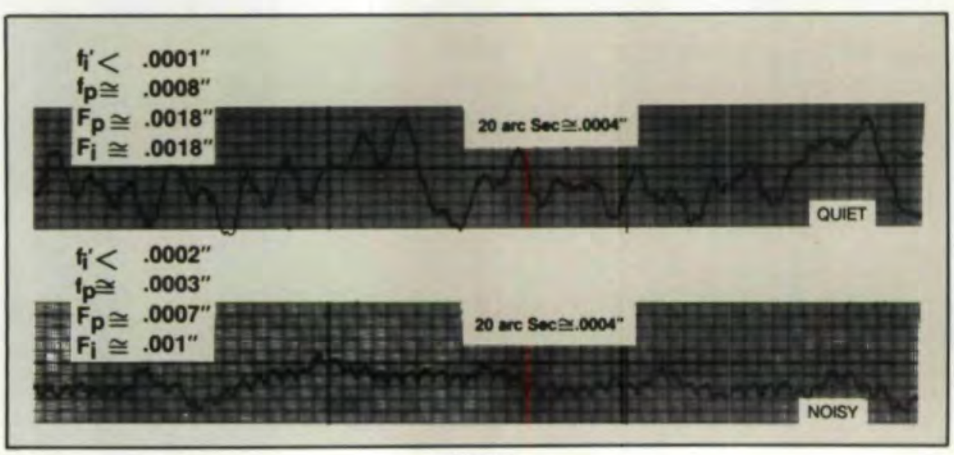

Fig. 10

The other pair was an experimental ground pair with very low total transmission error, but with a very regular high tooth to tooth error (.0002"). This pair was noisy in the vehicle at first and fourth harmonics of mesh frequency. In this case, the vehicle was a van type, which is typically sensitive to excitation due to structural dynamics.

(2) NOISE: Fig. 11 shows two lapped hypoid rear axle sets. Fig. 11a was acceptable in the vehicle and Fig. 11b was a reject because of noise due to the relatively high tooth to tooth transmission error.

(3) ACCURACY: Fig. 12 shows sets of ground high reduction gears used in the indexing spindle of a machine tool. Fig. 12a shows an unacceptable pair with excessive pinion runout (.0002"). Fig. 12b shows the next grind after improving the runout. In this example, it is no longer possible to detect a systematic error from gear geometry.

(4) ACCUMULATED PITCH VARIATION VS. RUNOUT: The last case is really two different sets of gears illustrating two aspects of Runout and Accumualted Pitch Variation (Fig.13). These are sets of final drive helicals used in the transaxle of a front wheel drive passenger car. The problem is related to a low frequency vibration in the vehicle, caused by once per revolution errors in the pinion.

Set number one (high accumulated pitch variation) caused excessive vibration in the vehicle. A double flank composite test accepted the part with .0025" pinion total composite error. However, the single flank test showed .0135" pinion total transmission error. In this case, the current pinion production test accepted a bad part.

Set number two (high runout) was acceptable in the vehicle as far as low frequency vibration. In this example, the double flank test rejected it because of a pinion total composite error of .009" while the single flank test still showed an acceptable amount of .003" pinion total transmission error. In this example, the current double flank production test rejected a part that should have been passed on to assembly.

In the two cases above, it is evident that double flank composite inspection does not correlate well to the application. On the other hand, single flank composite measurement of transmission error does.

Bibliography

1. SMITH, R. E., "What Single Flank Measurement Can Do For You." AGMA Paper No. 84FTM2. Fall Technical Meeting, 1984.

(continued on page 33)

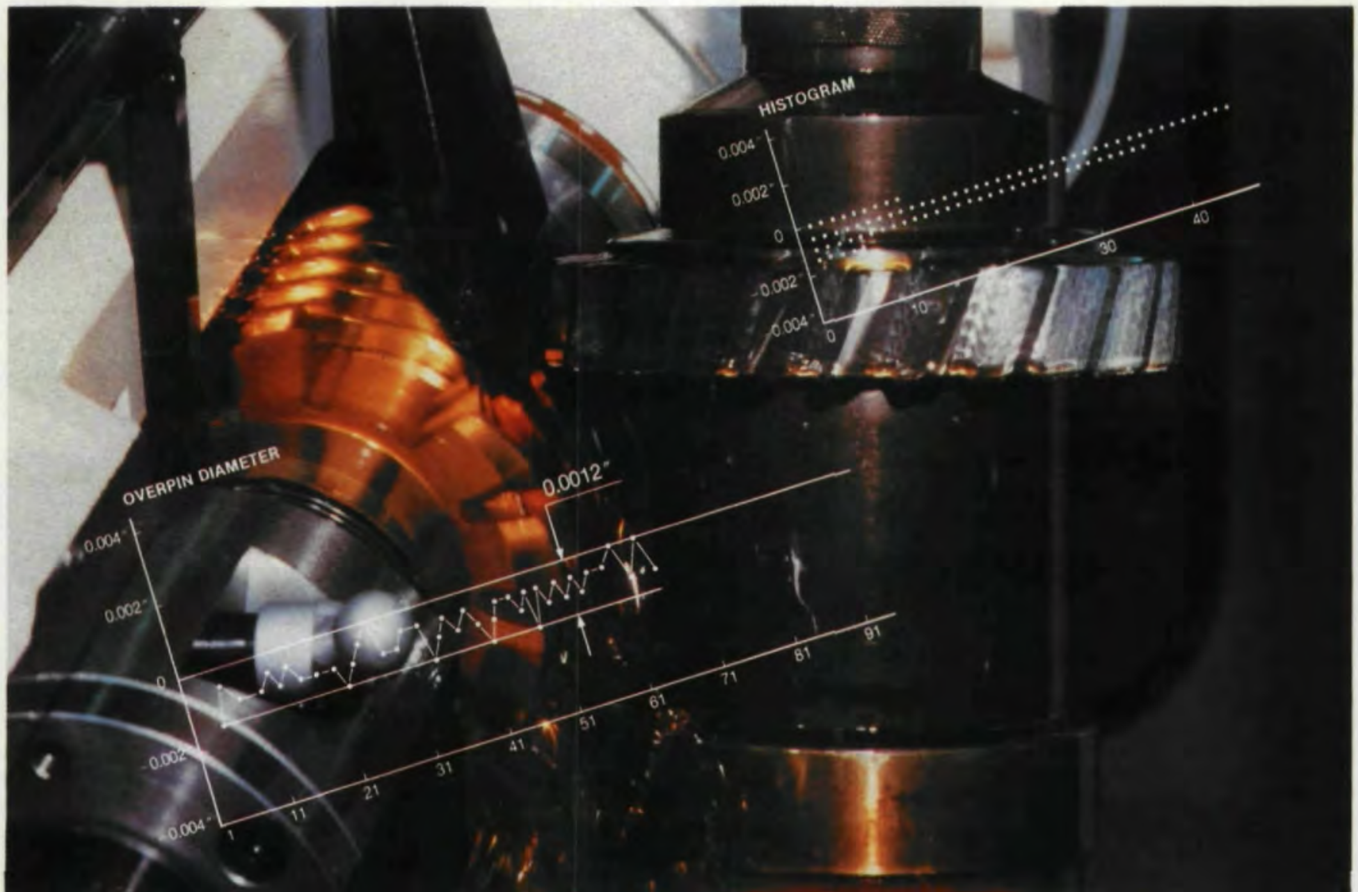

CAN YOU GET CONSISTENT OVERPIN DIAMETER OF 0.0012″ FROM COLD START?

You can, with Mitsubishi's new GA-Series Gear Hobbers!

Here's the reason why you can get such a consistent accuracy over hours of continuous running. To maintain the thermal stability of the machine, the hydraulic oil is maintained to a constant temperature by a refrigerating unit and the unit is isolated from the machine. The 36″ wide 3-runway bed and heavy duty ball screws also plays a big role in maintaining high accuracy.

Not only is the machine accurate but also can withstand heavy duty cuts due to the robust construction of the machine and an AC servo motor driven direct hob drive mechanism. A hydraulically controlled backlash eliminator on the indexing table permits "reverse hand conventional cutting" which gives 4 to 5 times more cutter life on your tools.

Another prominent feature of the machine is the conversational "MENU" programming. Just key in the gear and hob data and select the type of material you are going to cut. The computer of the CNC will do the rest for you. No calculation of cutter path or selection of cutting parameters.

Needless to say, with a full CNC machine, the changeover time can be reduced to a maximum of 90%.

These are only a part of what our GA-series can do for you. For more information, write to our Bensenville office below or call, area code 312-860-4220 NOW!

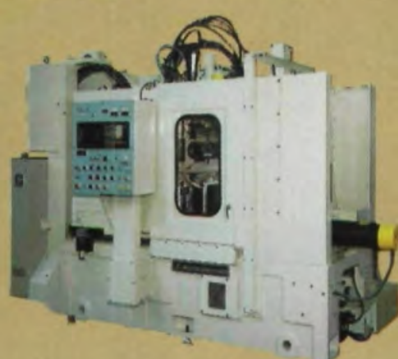

SPECIFICATIONS

	GA250NC	GA40CNC
Maximum part diameter	10″	16″
Maximum DP	4	4
Maximum radial travel	8.26″	10″
Maximum axial travel	10.6″	10.6″
Worktable diameter	8.45″	16.5″
Hob speed range	200～600rpm	200～600rpm
Hob drive motor	10hp	10hp

MITSUBISHI HEAVY INDUSTRIES, LTD.
5-1, Marunouchi 2-chome, Chiyoda-ku, Tokyo, Japan
Cable Address: HISHIJU TOKYO

Mitsubishi Heavy Industries America, Inc.
873 Supreme Drive, Bensenville, IL 60106 Phone: (312) 860-4220

CIRCLE A-9 ON READER REPLY CARD

SINGLE FLANK DATA ANALYSIS . . .
(continued from page 31)

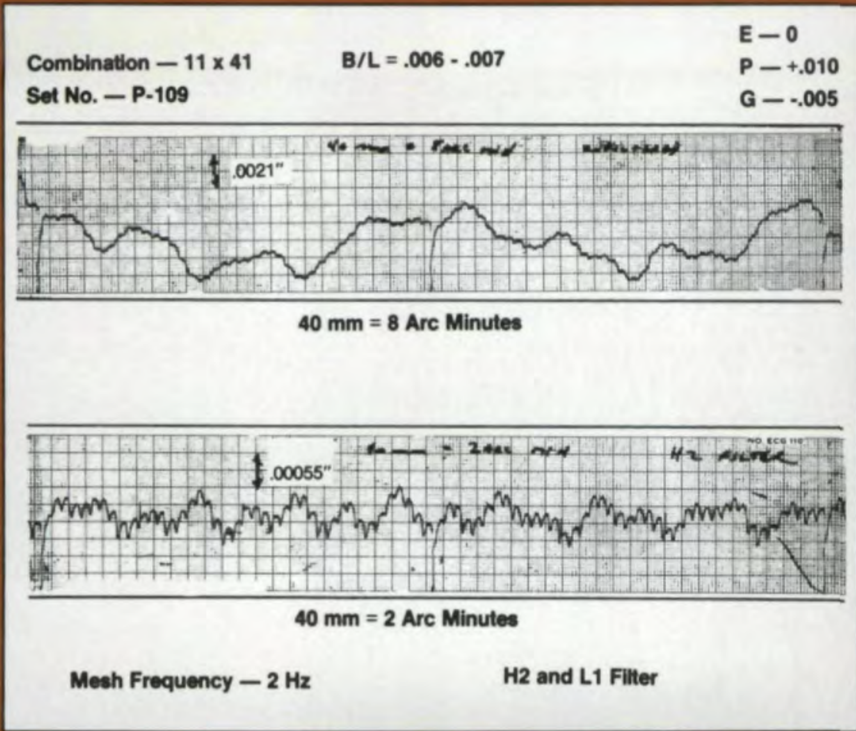

Fig. 11A – (Left) Acceptable lapped hypoid rear axle.

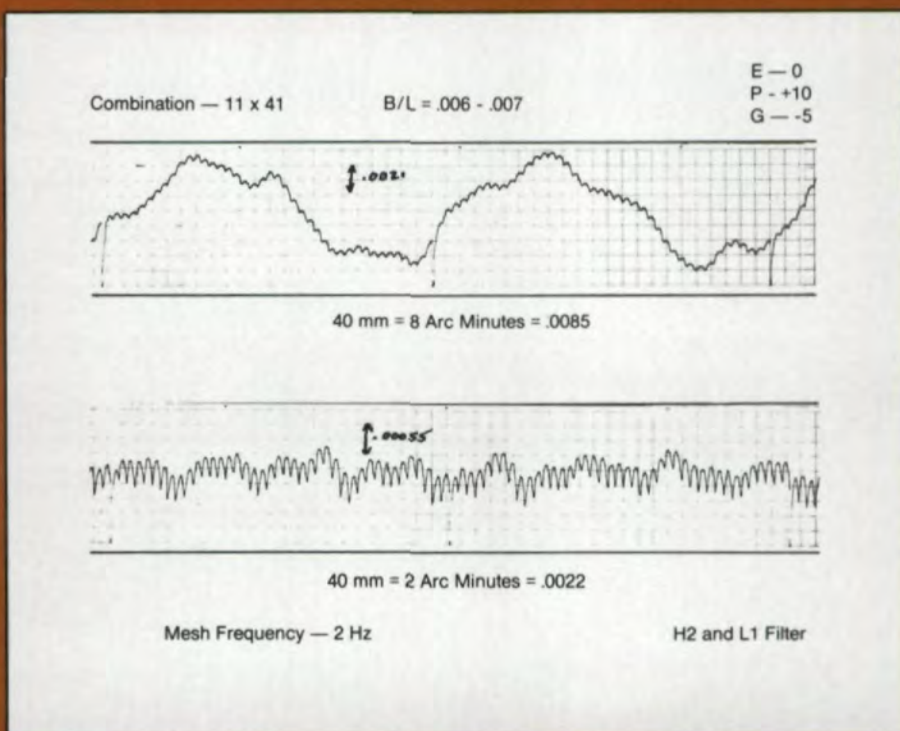

Fig. 11B – (Right) Rejected because of noise due to the relatively high tooth to tooth transmission error.

Fig. 12A – (Below) Pair with unacceptable runout.

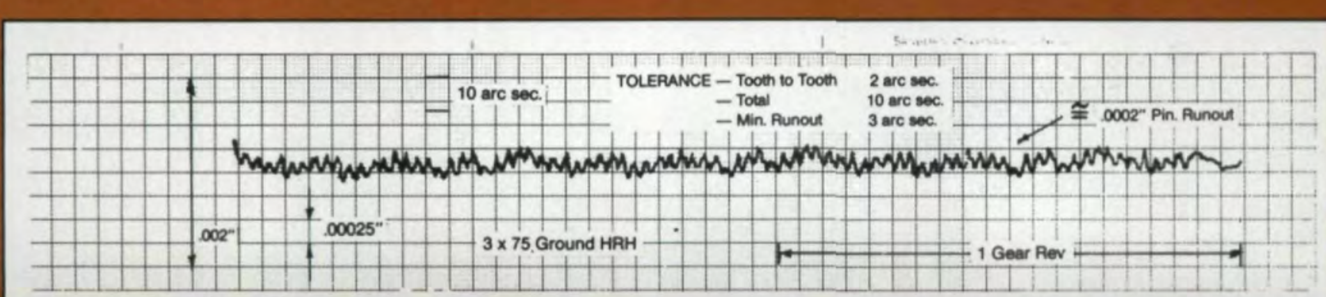

(continued on page 34)

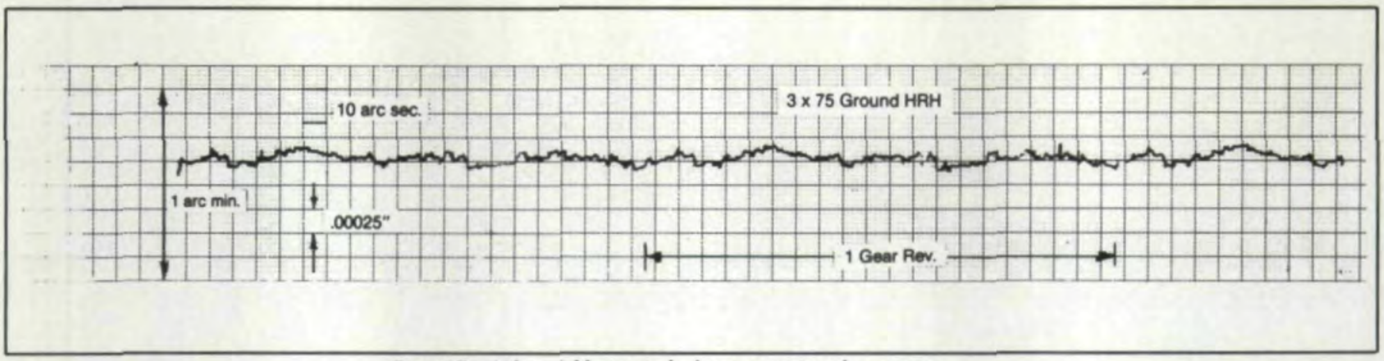

Fig. 12B – (Above) Next grind after improving the runout.

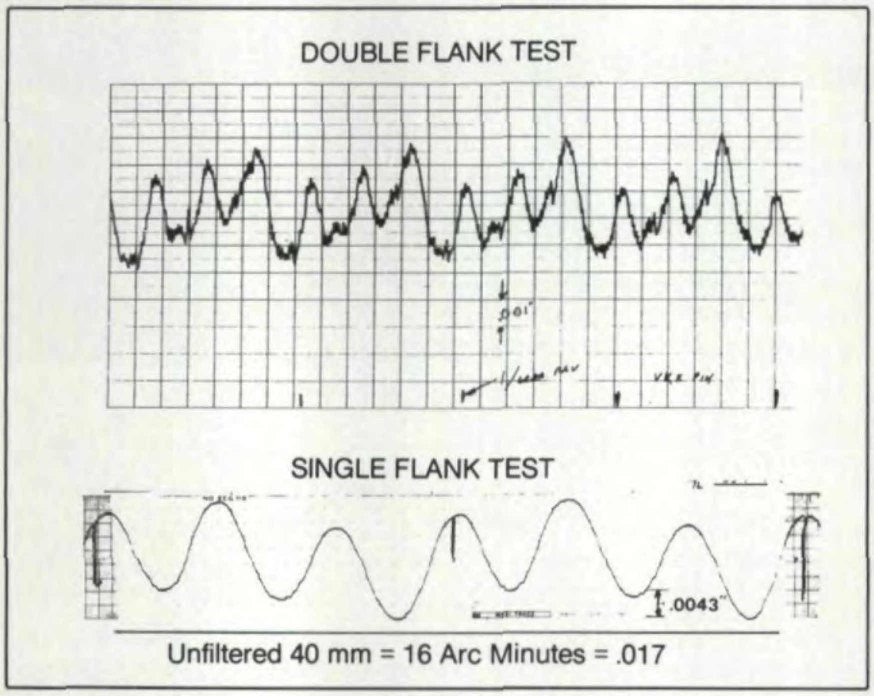

Fig. 13 – (Left) Set number one – high accumulated pitch variation

Fig. 13 – (Below) Set number two – high runout

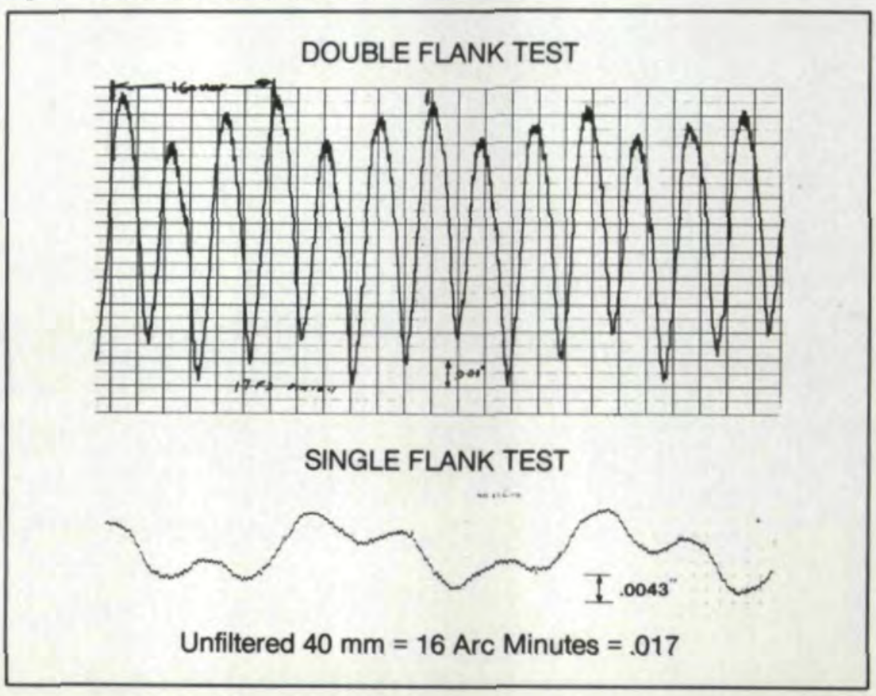

2. MUNRO, R. G., "Effect of Geometrical Errors on the Transmission of Motion Between Gears," Proc. I. Mech. E., Vol. 184 (1969-1970), Pt30, p.79.

3. MARK, W. D., "The Transfer Function Method for Gear System Dynamics Applied to Conventional and Minimum Excitation Gearing Designs," NASA Contractor Report 3626, 1982, pp. 2-3.

4. SMITH, R. E., "Single Flank Testing of Gears," Gear Technology, Vol. 1, No. 1, June/July 1984.

5. SMITH, J. D., "Gears and Their Vibration," Marcel Dekker 1983, p. 95.

E-2 ON READER REPLY CARD

New Techniques for Aligning and Maintaining Large Ring Gears

M. Antosiewicz
The Falk Corporation
Milwaukee, Wisconsin

Abstract

This paper presents two new techniques for aligning and maintaining large ring gears. One technique uses the "Operating-Temperaures" in the mesh of a ring gear set to evaluate the relative distribution of load across the face of the gearing. The other uses "Stop-Action" photography to record the surface condition and lubricant film on the pinion teeth. These techniques are recommended for use in conjunction with conventional maintenance procedures. Combined they optimize the gear set performance at the time of initial installation and then for the life of the gearing if they are used during subsequent maintenance procedures.

INTRODUCTION

The "Operating-Temperatures" alignment and the "Stop-Action" photography techniques have been under development at Falk for the last 5 to 6 years. Both have been rigorously tested on well over 100 different ring gear sets from various industrial applications. The gearing ranged up to 35 feet in diameter, 31 inches of face, and had pitches as course as ¾ DP. The techniques and the instrumentation required to use them are described in this paper. Also presented is some recent work which utilizes these procedures and interprets the results.

ALIGNMENT

Conventional Alignment Methods

There are basically three conventional methods which are used for aligning ring gear sets. These are presented here to provide a reference for comparison with the "Operating-Temperatures" method. The first uses feeler gages to measure the clearance at each end of the face, between the load flanks of the gear teeth when they are clean and contacting. With the second method, prussian blue, lamp black, or an equivalent is applied to several cleaned pinion teeth. That area of the pinion is then manually rotated into mesh with the gear and the teeth are bumped together transferring a contact pattern to the gear and the teeth are bumped together transferring a contact pattern to the gear where it can be inspected. The third method involves cleaning and dyeing the load flanks of several pinion and/or gear teeth with layout dye. The gearing is then operated under load for several hours, stopped and manually rotated to a convenient location to enable inspection of the dyed teeth. Areas on the teeth where dye is removed indicate the presence of contact.

These conventional techniques have certain disadvantages. The feeler gage and bump check methods indicate only static contact conditions. Since under load, the pinion, the gear, and associated equipment can deflect, twist and/or move through the internal clearance of the bearings, operating alignment may differ from static. The layout dye method offers a means of adjusting operating alignment to produce full face contact. Therefore, it can indicate when the entire face width of a tooth is carrying some load. However, it does not indicate whether the load intensity at one side of the face is greater than the load intensity on the opposite side.

Operating Temperatures Method

The "Operating-Temperatures" technique is a procedure, whereby, a uniform load intensity can be obtained across the entire face. This procedure is recommended for optimizing alignment after good initial alignment has been established using conventional methods. The basic premise behind the use of "Operating-Temperatures" is that misaligned gear sets experience non-uniform load intensity across the face of the gearing (Fig. 1). This variance in load intensity results in higher operating temperatures at the points of higher load. Therefore, misalignment will cause the operating temperature on one side of the face to be higher than on the other. As a result, equal temperatures at both ends of the face indicate a uniform load distribution and optimum alignment. Unequal temperatures indicate that the gear set may be misaligned with greater load intensity on the side of the face with the higher operating temperature.

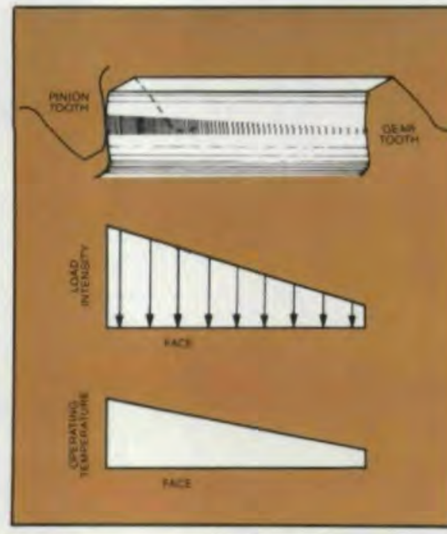

Fig. 1

Operating temperatures can be measured with either an infrared radiation thermometer, while the gearing is operating, or with a surface contact pyrometer immediately after stopping. (For

AUTHOR:

MR. M. ANTOSIEWICZ *is the Manager of Research and Technology at The Falk Corporation in Milwaukee, Wisconsin. He graduated from the University of Wisconsin with a B.S. in Engineering, and later he received a Masters in Business Administration. His activities at Falk include many aspects of gear design, manufacture and service.*

Fig. 2—Contact Pyrometer

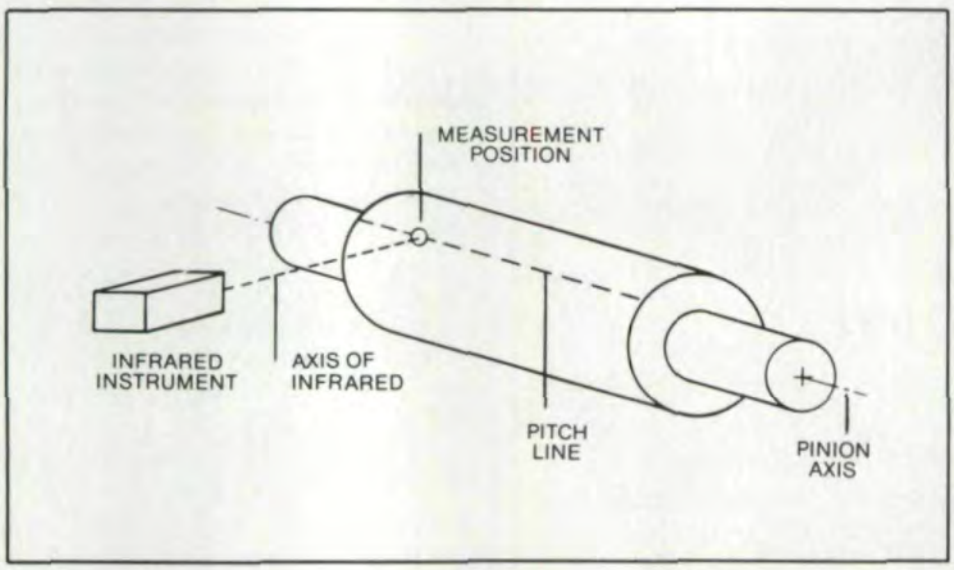

Fig. 3

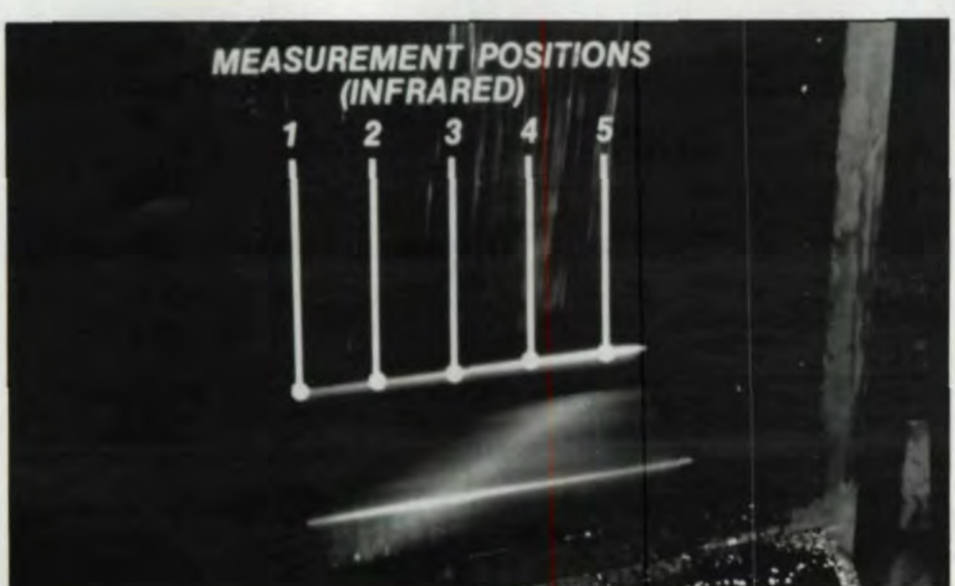

Fig. 4—Measurement Positions

typical instrument specifications, see Appendix A).

When using the surface contact pyrometer procedure, the probe is placed on the load flank at the pitch line of at least one tooth (Fig. 2). The measurements are taken directly through the lubricant film and immediately after stopping the gearing, since temperatures begin to change within minutes.

The infrared measurements are taken while the gearing is operating by pointing the infrared radiation measuring instrument perpendicular to the axis of the pinion and then aiming at the measurement position on the load flank along the pitch line (Fig. 3).

Examples of Evaluating Operating Temperatures

Five measurement positions were selected along the face of the mill pinion in Fig. 4. One measurement was taken at each end of the face . . . one at the center . . . and two additional midway between these points. It is very important that infrared measurements be taken along a straight horizontal line (as illustrated) in order to obtain the pitch line position. Deviations from this horizontal will produce erroneous data.

Temperature measurements can also be taken on the gear, however, the magnitudes of the temperatures and the temperature differentials across the gear face have been found to be smaller than those of the pinion and less sensitive to changes in alignment. Therefore, the pinion temperatures are considered more suitable for use in "Operating-Temperatures" alignment evaluations.

Fig. 5 illustrates the pinion temperature distribution of a gear set having optimum alignment. The temperature gradient, which is the temperature at Position 1 minus the temperature at Position 5, is zero indicating that the load intensity is the same on both ends of the pinion. Position 1 is taken toward the mill end of the pinion face.

Fig. 6 illustrates the temperature distribution of a gear set having poor alignment. The temperature gradient of the pinion is +40°F indicating that misalignment is producing higher load intensity on the mill side of the pinion. A negative gradient would indicate higher load toward the opposite side of the pinion face.

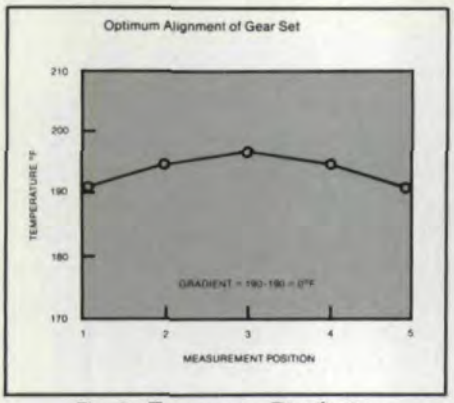

Fig. 5 – Temperature Distribution

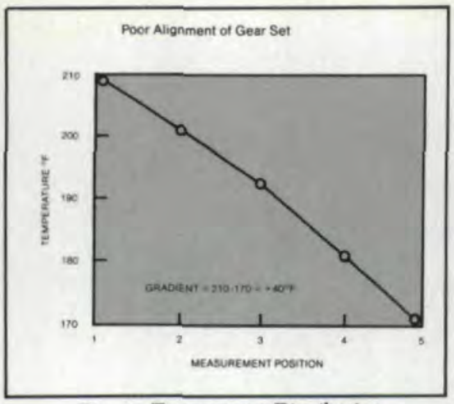

Fig. 6 – Temperature Distribution

Alignment Techniques

In addition to establishing a more uniform load distribution, the "Operating-Temperatures" technique offers two conveniences. First, when using the pyrometer, it is not necessary to connect an inching drive and rotate the gearing to view the contact patterns. Second, infrared techniques are able to sense the temperatures without stopping the mill.

The major limitation to using temperatures is that the surface condition of the teeth might influence the temperature and cause a false indication of alignment. Therefore, the presence of severe surface distress, recent scoring, wear pads, high points on the teeth, or other profile disturbances, should be considered when interpreting the temperatures.

Instrumentation

Both the surface contact pyrometer and the infrared instrument have advantages and limitations. The pyrometer has the advantage of accurate temperature measurement and simplicity of use. It has the disadvantage that the gearing must be stopped and, since temperatures begin to shift rapidly after stopping, only one or possibly two teeth can be measured.

Infrared has the advantage that the temperatures are measured during actual operating conditions. The temperatures recorded are, therefore, not changing with time as for the pyrometer. Also, the infrared averages these operating temperatures over many teeth at a given measurement position and, therefore, represents an overall alignment rather than the alignment of one or two particular teeth.

The primary limitation of the infrared is that it must be calibrated for the infrared energy emittance or emissivity of the pinion. This emissivity is essentially the relationship between the actual temperature of the pinion teeth and the amount of infrared energy tht is emitted for that temperature. It can be influenced by the type of lubricant, the lubricant film, and the tooth loads. Its value is determined by obtaining pyrometer measurements and then adjusting the infrared instrument to produce the same values. Experience has indicated that for various types of gear applications and lubricants the emissivity values may differ. However, the typical values appear to be in the order of 0.7 to 0.8. Since only relative and not absolute temperatures across the pinion face are desired to evaluate alignment, a value of 0.7 or 0.8 may be used and the measured temperatures considered nominal.

During the last five to six years, Falk has studied the gearing of over 100 different ring gear sets. The study was based primarily on mill gearing and has not been tested as thoroughly on kilns, because it is believed that the heat from the kiln along with the slow speed of the gearing might be misleading to infrared measurements. For mill gearing, detailed formulas have been developed to predict the alignment corrections required based on the measured temperature gradients. A study covering this is presented in Reference 1. However, for most mills, with only one pinion rotating out of mesh and located approximately 20° to 30° below the mill horizontal, equation 1 gives the approximate size of shim required to correct the alignment. This shim would be removed from or added under the appropriate pinion bearing to reduce the temperature and load intensity on the end of the face where it is the highest.

Equation 1

$$\text{Shim} = \frac{\text{Gradient}}{10{,}000} \quad \frac{\text{Bearing Span}}{\text{Face}} \quad \frac{\text{Design Load}}{\text{Operating Load}}$$

Example:

Consider a 3000 horsepower mill with a single pinion having a 39°F temperature gradient. The bearing span is twice the face width and the mill is operating at 2600 horsepower. The computed shim value would be:

$$\frac{39}{10{,}000} \quad 2 \quad \frac{3{,}000}{2{,}600} \quad = .009''.$$

Therefore, a .009" shim would be added or removed from under the appropriate bearing to reduce the load intensity on the high temperature end of the pinion.

Once an alignment correction is made, the mill should be allowed to operate for at least twenty hours in order to reach its steady state operating temperatures. The alignment should then be rechecked to determine whether further adjustments are necessary. Generally, when a gradient of 15°F or less is obtained, a satifactory alignment has been reached.

Stop Action Photos

The illustration above describes the surface condition and lubricant film on the pinion teeth of a ring gear set. It is a "Stop-Action" photo taken while the gearing was operating and provides a permanent detailed description of the tooth surface condition and the lubricant film existing on the pinion at the time the photo was taken. Surface distress such as scuffing, pitting and wear can readily be detected. By observation of the lubricant film, misalignment and lubricant contamination can at times be found. When "Stop-Action" photographs are used in conjunction with "Operating-Temperatures," misleading temperature rises and its cause can be identified. An example would be high temperatures due to localized scuffing when a lube spray nozzle fails.

The advantage of the "Stop-Action" photo is that it can be obtained with minimal effort, simple camera equipment, and most importantly, without stopping the gearing and interrupting production. It contains information useful to maintenance and engineering personnel for evaluating the performance history of the gearing and for detecting the need for corrective actions. It is also a means for recording and communicating tooth conditions and lubricant films to mill builders and gear manufacturers for review and appraisal.

The ability of "Stop-Action" photos to capture the tooth surface condition and lubricant film is further illustrated in the Fig. 7 series. Fig. 7A is a "Stop-Action" photo taken of a mill pinion during operation just seconds before the gearing was stopped. Fig. 7B was taken a few seconds after the gearing had stopped. Some lubricant had dropped on the pinion from the gear above. Fig. 7C presents the cleaned teeth of the pinion. These photos indicate that the "Stop-Action" photo gives a good representation of the appearance of the lubricant film and tooth surface conditions as they would appear had the gearing been stopped for a visual inspection.

Fig. 8 illustrates the history documenting capability of "Stop-Action" photos. This series records the tooth surfaces of a particular pinion over a one year period. Initially the gearing was found to be scuffed and some pitting had occurred (Fig. 8A). Two months later (Fig. 8B), the condition was found to be improving. This improvement continued through the remainder of the year (Fig. 8C and 8D). Had the pitting become worse, corrective action could have been planned and nonscheduled downtime avoided. The significance of this series is that the photographs provide a far better history than memory, notes or sketches from which to make maintenance decisions.

Photographic Technique

The photographic equipment required to obtain "Stop-Action" photos is readily available, relatively inexpensive and simple to use. The camera is a 35 mm single lens reflex type having a 50 mm focal length lens. Stopping the motion of

Fig. 7—Operating Teeth vs. Static

7A Operating

7B Static

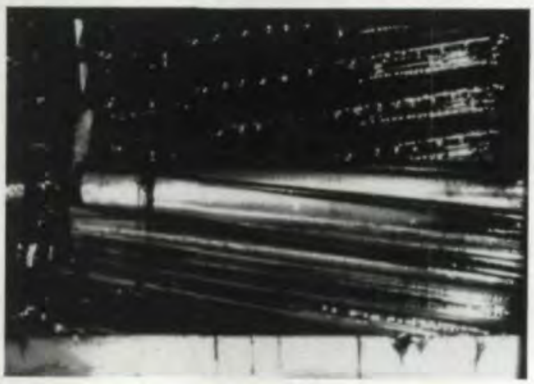

7C Cleaned Teeth

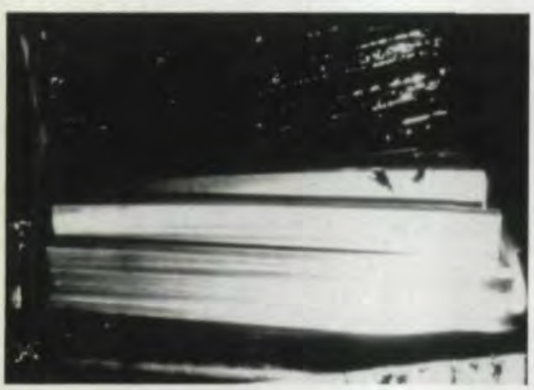

the pinion is accomplished with an automatic electronic flash having a guide number of about 100 (ASA100) or higher, and also a remote sensor which can be mounted on the camera hot shoe. Color slide film (ASA160 or ASA200) has worked well and is recommended. Print type film is nor recommended since the colors of the prints can be influenced during processing.

Fig. 9 illustrates the positioning of the camera and flash. The camera should be centered and focused on the load flank of the pinion teeth until the camera viewer is filled by the pinion teeth. The flash should be set to automatic operation for an aperture of approximately f5.6. The camera lens should be set to the same aperture. The remote sensor should be positioned on the camera hot shoe and the flash oriented at approximately 30° to the helix in order to minimize reflected glare from the tooth surface.

Once the proper camera and flash position is attained, the shutter button is depressed. This opens the camera lens. The flash will then fire in approximately 1/5,000 to 1/30,000 of a second stopping the action of the gearing like a stroboscope and exposing the film. The camera shutter then closes and the "Stop-Action" picture is obtained.

Both "Operating-Temperatures" alignment and "Stop-Action" photography provide useful information regarding the operation of large ring gearing. Presented here are some ways that these two techniques have been used, both individually and in combination, to gain more insight into ring gear alignment and lubricant films. Presented first, is a discussion of transient shifts in the alignment of a mill gear set from start-up to steady-state conditions. This is followed by an investigation into the influences of lubricant type, viscosity and operating temperature on the appearance of the lubricant as captured in "Stop-Action" photos.

Alignment Transient Shifts

As previously indicated, static alignment and operating alignment may be different. One possible source of this difference, (discovered through the use of infrared) is that the alignment of a mill gear set can shift over a period of time as the mill progresses from a stopped condition to its steady-state operating conditions. This transient type shift was encountered in hot air type dry process mills.

An example of the temperature gradients of such a mill is given in Fig. 10. Here the gradient of the mill pinion shifted from −21°F to +18°F over a period of approximately twenty hours. This represents a 30°F shift in gradient which, for that particular mill, corresponded to a .009" change in alignment over the pinion bearing span. It is suspected that this shift was the result of thermal growth of the mill as it came up to normal operating temperatures.

A wet process taconite grinding mill is also included in Fig. 10 for comparison. For that mill, the steady state operating gradient was reached within approximately one-half hour with no evidence of any alignment shift.

At any rate, to be certain steady-state operating temperatures have been reached, it is recommended that the mill be operated for approximately twenty hours prior to taking "Operating-Temperatures".

Lubricant Films

"Stop-Action" photography, besides recording pinion tooth surface conditions, describes the operating lubricant films on the pinion tooth. Falk experience indicates that these films can vary significantly depending upon the type of mill and the operating conditions. These visual differences in lube film prompted exploratory tests regarding the possible influences of lubricant type, viscosity and operating temperature on the appearance of the film.

Lubricant Type

The lubricants investigated were asphatic base, residual type compounds typically used for ring gearing. Their viscosities ranged from 4,750 SSU to 17,200 SSU at 210°F undiluted. They were produced by various manufacturers. None of the lubricants had a large percentage of solid lubricant additives.

Fig. 8 – Gear Performance History

8A Initial Photo

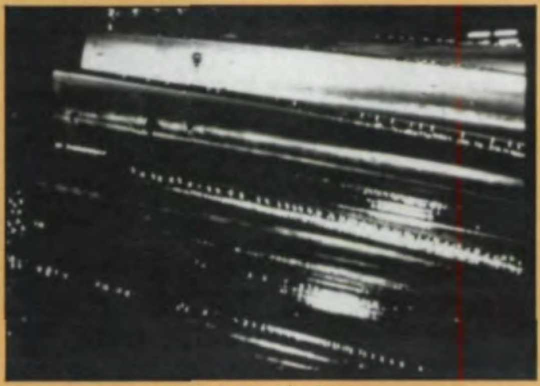

8B 2 Months Later

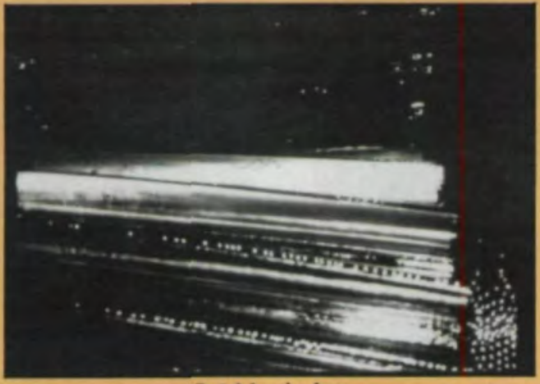

8C 8 Months Later

8D 1 Year Later

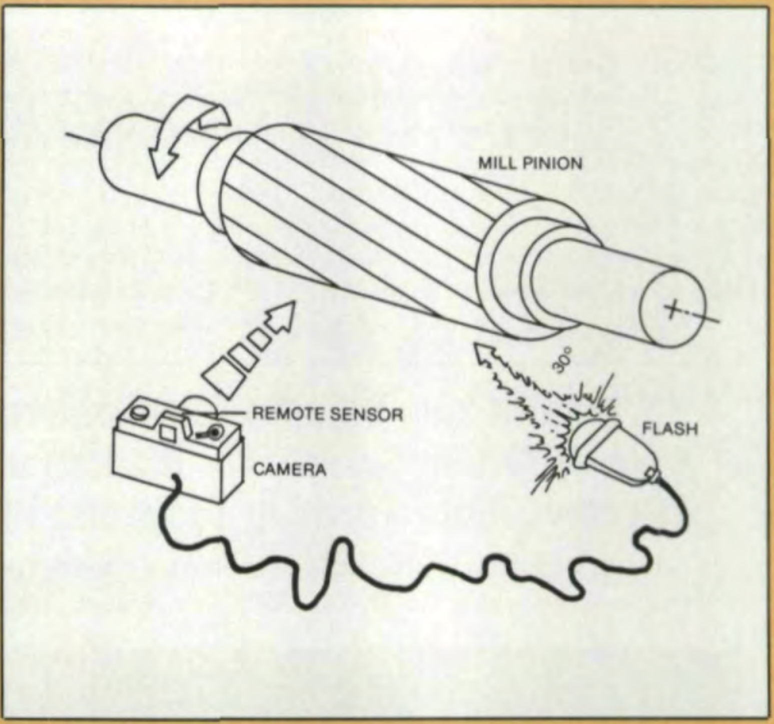

Fig. 9 – Camera and Flash Positions

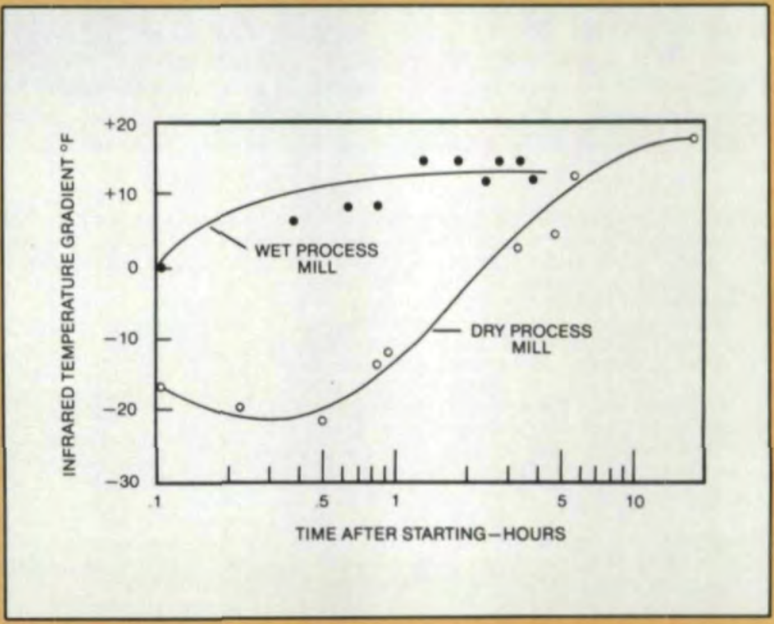

Fig. 10 – Transient Shift in Alignment

Since differences in the lubricant films on photos appeared as changes in darkness and color, it was important to determine whether the color of the lubricant varied with film thickness or differed between lubricants of different manufacturers. A laboratory test was performed. It involved placing a piece of ½" plate glass over a ground steel bar, which had been coated with lubricant and had a .002" step in the bar (Fig. 11). This step produced a space between the bar and the plate glass that increased from 0" to .002" over the 3" length of the step and which was filled with lubricant. The relation between lubricant film thickness and its color could then be observed through the glass and photographed.

Inspections of the glass and the plate indicated that both were flat to within less than .0001" over the area of contact. Before applying the lubricant to the steel plate, the glass, the lubricant and the plate were heated to approximately 190°F to drive any diluent from the lubricant and achieve a uniform temperature. The photography lighting was identical for each lubricant photo. It was also very similar to the lighting used for photographing operating mill pinions.

The results of this testing show that the color distribution with film thickness is very similar for each lubricant. Additional tests in which the lubricants were allowed to cool to room temperature (70°F) indicated that the color of the lubricant did not change with temperature.

These exploratory tests suggest that residual type lubricants are basically the same color and that lubricant film color might be used to estimate or compare lube film thicknesses.

Lubricant Viscosity

The glass plate test also indicated that changing viscosity within the 4,750-17,200 SSU range did not significantly influence the relationship between color and film thickness of the lubricants tested. This observation was used in the evaluation of a field test where these same lubricants had been individually applied to the same mill pinion. Adequate time had been allowed for each lubricant to establish its own film. The resultant films were very similar. The pinion operating temperatures, which were monitored with infrared and surface contact temperature instruments, remained essentially constant (184°F to 190°F) for all lubricants tested. The indication of this test was that the change in non-diluated viscosity within the 4,750 to 17,200 SSU range, which is typical for residual compounds, did not significantly influence the lubricant film appearance.

Operating Temperature

From the previous testing, the variance in lubricant film, between different pinions, does not appear to be significantly related to the specified viscosity or manufacturer of the lubricant for the viscosities and lubricant types tested. The third parameter investigated, temperature, was found to have significant influence. This was observed in a field test where the lubricant film was monitored from the time the mill started, at ambient temperature (80°F), until it reached its

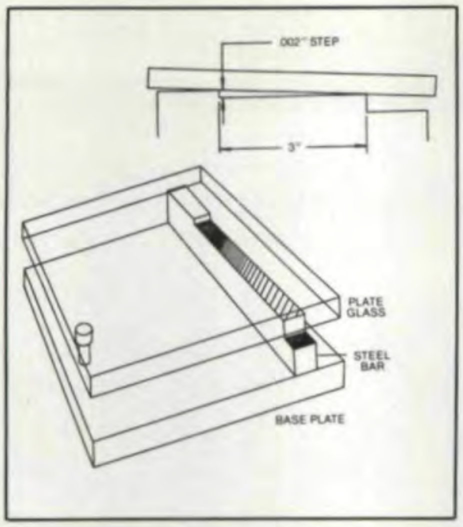

Fig. 11 – Lube Film Test Setup

Fig. 12 – Lubricant Film Color Change After Start-Up (Start 70°F Final 179°F)

12A ½ Hr. After Start

12B 2 Hr. After Start

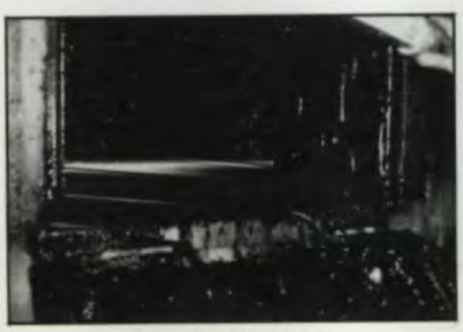

12C 6 Hr. After Start

12D 24 Hr. After Start

normal operating temperature of 179°F. Fig. 12 describes the change in film at various times after startup and shows that the lubricant film becomes lighter in color as the temperature increases. From the glass plate test, this would indicate that the film thickness is also decreasing.

The relationship between lubricant film and operating temperature is further illustrated in Fig. 13. Here, four mill pinions from different applications, using different lubricants, are shown along with their corresponding operating temperatures. Again, the color of the lubricant film becomes lighter, indicating a thinner film as the operating temperature increases. This agrees with the results in Fig. 12. In general, similar results were found on other gearing where both photos and temperatures were obtained.

CONCLUSION

This paper has presented two new techniques for aligning and maintaining large ring gears. The techniques are particularly beneficial because they can be utilized while the gearing is operating and, therefore, do not interfere with production. The unique advantage of the "Operating-Temperatures" technique is that it indicates relative load intensity across the face of the gearing and not just contact. The "Stop-Action" photo captures the tooth surface condition and lubricant film on the teeth of an operating gear set. This is accomplished with readily available, simple to use and relatively inexpensive photography equipment. The photos provide a far better history than memory, notes or sketches from which to make maintenance decisions.

Both these techniques are recommended for use by engineering and maintenance personnel for evaluating gearing condition and performance. They are also recommended for consideration when taking necessary corrective action during the life of the gearing.

Reference

1. ANTOSIEWICZ, M., "The Use of Mill Gear Operating Temperatures for Alignment Evaluation," IEEE Cement Industry 21st Technical Conference, Tarpon Springs, Florida May 1979.

Fig. 13 – Lubricant Film vs. Lubricant and Temperature

13A Whitmore Med. 147°F.

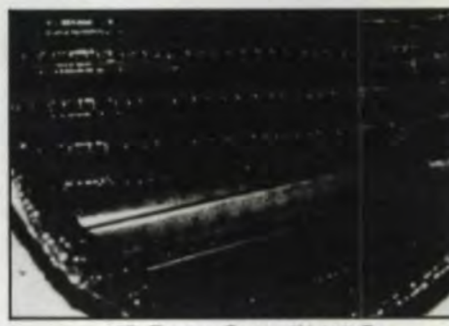

13B Texaco Crater 5X 165°F.

13C Mobiltac C 180°F

13D Mobiltac C 195°F

(Appendix continued on page 48)

Material Selection and Heat Treatment
Part II
Metalurgical Characteristics

National Broach & Machine Division of Lear Siegler
Mt. Clemens, MI 48044

(This article is a continuation. Part I was presented in the July/August 1985 issue of GEAR TECHNOLOGY.)

Metallurgical Characteristics*

The approximate tensile strength of any steel is measured by its hardness, Table 1. Since hardness is determined by both chemical composition and heat treatment, these are the two important metallurgical considerations in selecting gear steels.

Chemical Composition

Hardenable gear steels are of two types: through-hardenable or case-hardenable. Through-hardenable steels contain alloying elements and usually have carbon content ranging from about 0.40 to 0.50-percent to give the desired hardness. Steels for case-hardening may or may not contain alloying elements, but have lower carbon content (usually less than 0.25-percent). The lower carbon content permits development of high surface hardness while retaining a softer, more ductile core.

An alloy steel, Table 2, is a type to which one or more alloying elements have been added to give it properties that cannot be obtained in carbon steel. Chromium is one of the most versatile and widely used alloying elements. It produces corrosion and oxidation resistance, and induces high hardness and wear resistance. It also intensifies the action of carbon, increases the elastic limit, increases tensile strength, and increases depth of hardness penetration.

Nickel increases shock resistance, elastic limit, and tensile strength of steel. Nickel steels are particularly suitable for case-hardening. This results in their frequent use for aircraft gears where strength-to-weight ratio must be high. The strong, tough case obtained with nickel steels combined with good core properties provides exceptional fatigue and wear resistance. Simplified hardening procedures and low distortion during heat treatment result from lower transformation temperature ranges and the relatively small difference between case and core transformation temperatures.

Molybdenum increases hardenability of steels and has a significant effect on softening of steels at tempering temperatures. It markedly retards softening of the hardened martensite at tempering temperatures above 450F.

**Implemented and reviewed by Harold A. Maloney, plant metallurgist, Clark Equipment Co.*

Vanadium is used as an alloying element in steels for two reasons. First is the effect on grain size at elevated temperatures. Vanadium stabilizes the fine grain structure of austenitized steels and permits retention of excellent ductility and impact resistance while developing high tensile and yield strengths. The second reason is the ability to form carbides which remain stable at elevated temperatures.

Hardenability is the property of a steel which determines the depth and distribution of the hardness induced by quenching. The higher the hardenability of a steel, the greater the depth to which the steel can be hardened and the slower the quench which can be used. Hardenability should not be confused with hardness or maximum hardness which can be obtained by heat treatment, since that depends almost entirely

Table 1 – Approximate Tensile Strength for Equivalent Hardness Numbers of Steel

Brinell Indentation Diameter, mm	Brinell Hardness Number, 3000-Kg 10 mm Tungsten Carbide Ball	Rockwell Hardness Number B-Scale 100-Kg Load 1/16 in. Ball	Rockwell Hardness Number C-Scale 150-Kg Load Brale Penetrator	Vickers Diamond Pyramid Hardness Number	Shore Scleroscope Hardness Number	Approx. Tensile Strength 1000 p.s.i.
2.25	745	—	65.3	840	91	—
—	710	—	63.3	780	87	—
2.35	682	—	61.7	737	84	—
2.40	653	—	60.0	697	81	—
2.45	627	—	58.7	667	79	—
2.50	601	—	57.3	640	77	—
2.55	578	—	56.0	615	75	—
2.60	555	—	54.7	591	73	298
2.65	534	—	53.5	569	71	288
2.70	514	—	52.1	547	70	274
2.75	495	—	51.0	528	68	264
2.80	477	—	49.6	508	66	252
2.85	461	—	48.5	491	65	242
2.90	444	—	47.1	472	63	230
2.95	429	—	45.7	455	61	219
3.00	415	—	44.5	440	59	212
3.05	401	—	43.1	425	58	202
3.10	388	—	41.8	410	56	193
3.15	375	—	40.4	396	54	184
3.20	363	—	39.1	383	52	177
3.25	352	(110.0)	37.9	372	51	170
3.30	341	(109.0)	36.6	360	50	163
3.35	331	(108.5)	35.5	350	48	158
3.40	321	(108.0)	34.3	339	47	152
3.45	311	(107.5)	33.1	328	46	147
3.50	302	(107.0)	32.1	319	45	143
3.55	293	(106.0)	30.9	309	43	139
3.60	285	(105.5)	29.9	301	—	136
3.65	277	(104.5)	28.8	292	41	131
3.70	269	(104.0)	27.6	284	40	128
3.75	262	(103.0)	26.6	276	39	125
3.80	255	(102.0)	25.4	269	38	121
3.85	248	(101.0)	24.2	261	37	118
3.90	241	100.0	22.8	253	36	114
3.95	235	99.0	21.7	247	35	111
4.00	229	98.2	20.5	241	34	109
4.05	223	97.3	(18.8)	234	—	104
4.10	217	96.4	(17.5)	228	33	103
4.15	212	95.5	(16.0)	222	—	100
4.20	207	94.6	(15.2)	218	32	99
4.25	201	93.8	(13.8)	212	31	97
4.30	197	92.8	(12.7)	207	30	94
4.35	192	91.9	(11.5)	202	29	92
4.40	187	90.7	(10.0)	196	—	90
4.45	183	90.0	(9.0)	192	28	89
4.50	179	89.0	(8.0)	188	27	88
4.55	174	87.8	(6.4)	182	—	86
4.60	170	86.8	(5.4)	178	26	84
4.65	167	86.0	(4.4)	175	—	83
4.70	163	85.0	(3.3)	171	25	82
4.80	156	82.9	(0.9)	163	—	80
4.90	149	80.8	—	156	23	—
5.00	143	78.7	—	150	22	—
5.10	137	76.4	—	143	21	—
5.20	131	74.0	—	137	—	—
5.30	126	72.0	—	132	20	—
5.40	121	69.8	—	127	19	—
5.50	116	67.6	—	122	18	—
5.60	111	65.7	—	117	15	—

The indentation and hardness values in the foregoing table are taken from Table 2, Approximate Equivalent Hardness Numbers for Brinell Hardness Numbers for Steel, pages 122 and 123 of 1952 SAE Handbook, Society of Automotive Engineers, Incorporated.

The values shown in parentheses are beyond the normal range of the test scale and are given only for comparison with other values.

Courtesy Republic Steel Corp.

Table 2 – Basic AISI and SAE Numbering System for Steels

Numerals and Digits	Type of Steel and Average Chemical Contents, %
	CARBON STEELS
10XX	Plain Carbon (Mn 1.00% max)
11XX	Resulphurized
12XX	Resulphurized and Rephosphorized
15XX	Plain Carbon (max Mn range—over 1.00—1.65%)
	MANGANESE STEELS
13XX	Mn 1.75
	NICKEL STEELS
23XX	Ni 3.50
25XX	Ni 5.00
	NICKEL-CHROMIUM STEELS
31XX	Ni 1.25; Cr 0.65 and 0.80
32XX	Ni 1.75; Cr 1.07
33XX	Ni 3.50; Cr 1.50 and 1.57
34XX	Ni 3.00; Cr 0.77
	MOLYBDENUM STEELS
40XX	Mo 0.20 and 0.25
44XX	Mo 0.40 and 0.52
	CHROMIUM-MOLYBDENUM STEELS
41XX	Cr 0.50, 0.80 and 0.95; Mo 0.12, 0.20, 0.25 and 0.30
	NICKEL-CHROMIUM-MOLYBDENUM STEELS
43XX	Ni 1.82; Cr 0.50 and 0.80; Mo 0.25
43BVXX	Ni 1.82; Cr 0.50; Mo 0.12 and 0.25; V 0.03 minimum
47XX	Ni 1.05; Cr 0.45; Mo 0.20 and 0.35
81XX	Ni 0.30; Cr 0.40; Mo 0.12
86XX	Ni 0.55; Cr 0.50; Mo 0.20
87XX	Ni 0.55; Cr 0.50; Mo 0.25
88XX	Ni 0.55; Cr 0.50; Mo 0.35
93XX	Ni 3.25; Cr 1.20; Mo 0.12
94XX	Ni 0.45; Cr 0.40; Mo 0.12
97XX	Ni 0.55; Cr 0.20; Mo 0.20
98XX	Ni 1.00; Cr 0.80; Mo 0.25
	NICKEL-MOLYBDENUM STEELS
46XX	Ni 0.85 and 1.82; Mo 0.20 and 0.25
48XX	Ni 3.50; Mo 0.25
	CHROMIUM STEELS
50XX	Cr 0.27, 0.40, 0.50 and 0.65
51XX	Cr 0.80, 0.87, 0.92, 0.95, 1.00 and 1.05
501XX	Cr 0.50
511XX	Cr 1.02
521XX	Cr 1.45
	CHROMIUM VANADIUM STEELS
61XX	Cr 0.60, 0.80 and 0.95; V 0.10 and 0.15 minimum
	TUNGSTEN CHROMIUM STEELS
71XXX	W 13.50 and 16.50; Cr 3.50
72XX	W 1.75; Cr 0.75
	SILICON MANGANESE STEELS
92XX	Si 1.40 and 2.00; Mn 0.65, 0.82 and 0.85; Cr 0.00 and 0.65
	LOW ALLOY HIGH TENSILE STEELS
9XX	Various
	STAINLESS STEELS
	(Chromium-Manganese-Nickel)
302XX	Cr 17.00 and 18.00; Mn 6.50 and 8.75, Ni 4.50 and 5.00
	(Chromium-Nickel)
303XX	Cr 8.50, 15.50, 17.00, 18.00, 19.00, 20.00, 20.50, 23.00, 25.00
	Ni 7.00, 9.00, 10.00, 10.50, 11.00, 11.50, 12.00, 13.00, 13.50, 20.50, 21.00, 35.00
	(Chromium)
514XX	Cr 11.12, 12.25, 12.50, 13.00, 16.00, 17.00, 20.50 and 25.00
515XX	Cr 5.00
	BORON INTENSIFIED STEELS
XXBXX	B denotes Boron Steel
	LEADED STEELS
XXLXX	L denotes Leaded Steel

NOTE: "XX" after numbers or letters in table indicates carbon percentage; i.e. 1040 indicates 0.40 percent carbon.

From SAE Iron and Steel Handbook Supplement 30

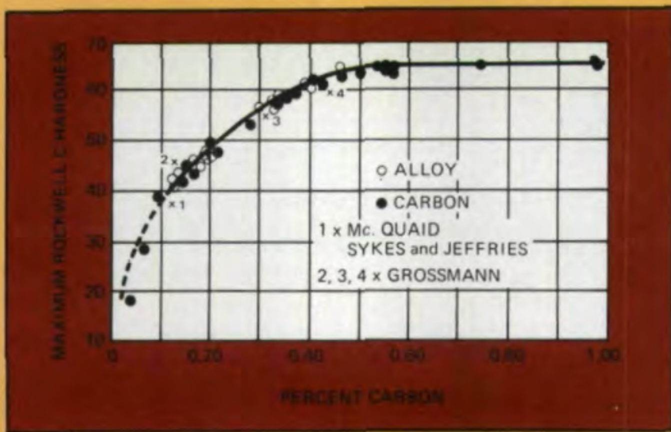

Fig. 1 – Relationship of maximum quenched hardness of alloy and carbon steels to carbon content. *Courtesy Republic Steel Corp.*

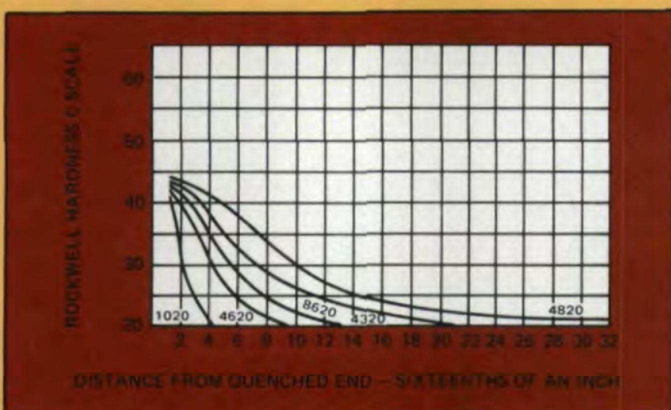

Fig. 2 – Comparative hardenability of 0.20-percent carbon alloy steels. *Courtesy Republic Steel Corp.*

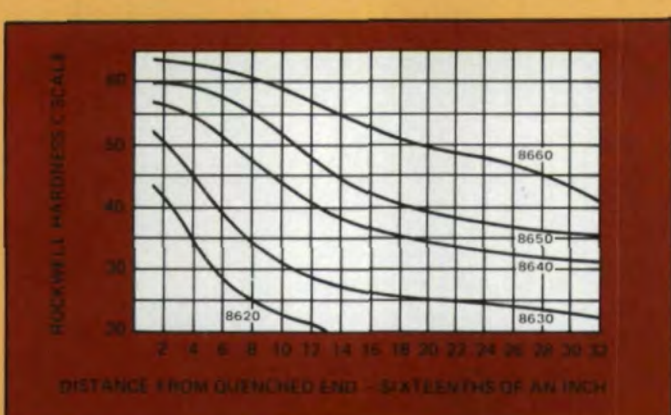

Fig. 3 – Comparative hardenability of 8600 Alloy Steels. *Courtesy Republic Steel Corp.*

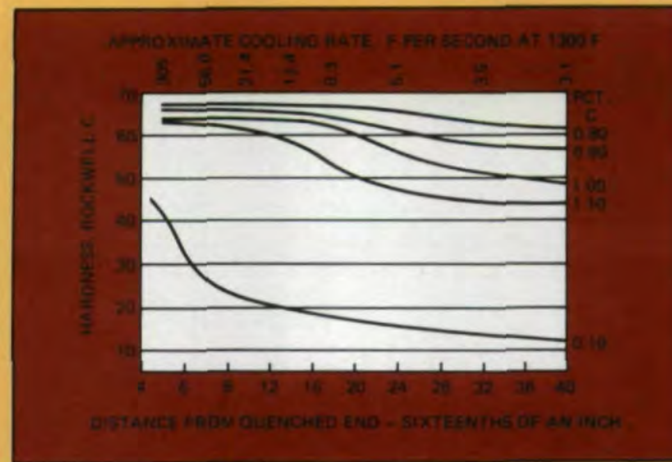

Fig. 4 – Curves showing that maximum hardenability of 8620 steel is achieved when case carbon concentration is at 0.80-percent carbon. *Courtesy Climax Molybdenum Co.*

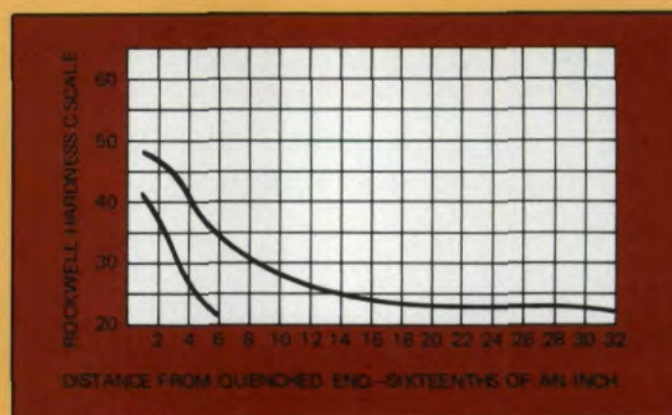

Fig. 5 – Hardenability upper and lower curve limits for 8620H steel. *SAE Iron and Steel Handbook Supplement 30.*

on carbon content, Fig. 1. Also, section thickness has considerable influence on the maximum hardness obtained for a given set of conditions; the thicker the section, the slower the quench rate will be. Variations in test bar hardenability curves for various 0.20-percent carbon and alloy steels is shown in Fig. 2. Similar hardenability curves for 8600 alloy steels with various carbon contents is shown in Fig. 3. Maximum hardenability of case-hardened 8620 steel is achieved, Fig. 4, when the case carbon concentration is 0.80-percent.

H-steels are guaranteed by the supplier to meet established hardenability limits for specific grades of steel. These steels are designated by an "H" following the composition code number, such as 8620H, Fig. 5. Hardenability of H-steels and a steel with the same chemical composition is not necessarily the same. Therefore, H-steels are often specified when it is essential that a given hardness be obtained at a given point below the surface of a gear tooth.

E-5 ON READER REPLY CARD

Acknowledgement: *Reprinted from Modern Methods of Gear Manufacture, 4th Edition, published National Broach and Machine Division of Lear Siegler, Inc., 17500 Twenty Three Mile Rd., Mt. Clemens, MI 48044.*

CALCULATION OF SPUR GEAR TOOTH . . .

(continued from page 14)

12. TERAUCHI, Y., and NAGAMURA, K., "Study on Deflection of Spur Gear Teeth," *Bull. of JSME*, Vol. 24, No. 188, Feb. 1981, pp. 447-452.
13. FORTIN, A., "Application de la méthode des potentiels complexes aux calculs des déplacements dans les engrenages droits," M.Sc. thesis, Laval University, Quebec, Canada, June 1983.
14. TIMOSHENKO, S. P., and GOODIER, J. N., *Theory of Elasticity*, McGraw-Hill, New York, 3rd ed., 1970.

E-1 ON READER REPLY CARD

CLASSIFIED

Rates: Classified Display—$100 per inch (minimum 3") Type will be set to advertiser's layout or *Gear Technology* will set type at no extra charge. **Word Count:** 35 characters per line, 7 lines per inch. **Payment:** Full payment must accompany classified ads. Mail copy to *Gear Technology*, P.O. Box 1426, Elk Grove Village, IL 60007. **Agency Commission:** No agency commission on classifieds. **Closing date:** Ads must be received by the 25th of the month, two months prior to publication. **Acceptance:** Publisher reserves the right to accept or reject classified advertisements at his discretion.

HELP WANTED

TECHNICAL CALENDAR

Sept. 16-18 1985 — Gear Noise Course
Ohio State University

This course will cover general noise measurements and analysis, causes of gear noise, gear reduction techniques, dynamic modelling, signal analysis and gear boxes. For further information contact: Mr. Richard D. Frasher, Director, Continuing Education, College of Engineering, 2070 Neil Ave., Columbus, Ohio 43210, (614) 422-8143.

Oct. 14-16 1985 — American Gear Manufacturers Fall Technical Meeting
Fairmont Hotel
San Francisco, CA

The AGMA Fall Technical Conference is an opportunity to keep abreast of the latest in technological developments, new standards of excellance, new engineering concepts, and new methods of manufacturing. This three day conference focuses on the best ideas from the best minds in the industry. To get more information on the AGMA's Fall Technical meeting, call (703) 684-0211, or write AGMA, 1500 King Street, Suite 201, Alexandria, VA 22314.

Nov. 19-21 1985 — Society of Manufacturing Engineers Gear Processing and Manufacturing Clinic, Detroit, Michigan.

SME's annual "Gear Processing and Manufacturing" clinic and tabletop exhibits will be held at The Dearborn Inn in Dearborn, Michigan November 19-21, 1985. Current technologies in the gear industry will be covered. J. Richard Newman, formerly of National Broach and Machine Division of Lear Siegler, and Carl S. Eckberg of Bourn & Koch Machine Tool Co., are co-chairing this three-day clinic. An evening of vendor tabletop exhibits will accompany the daily technical presentations. For further information on the clinic or the exhibits, contact Dianne Leverton at SME, 313/271-1500, extension 394.

March 17-19 1986 — International Conference on Austempered Ductile Iron, Ann Arbor, Michigan

HOB LENGTH EFFECTS . . .
(continued from page 19)

$$F'(Y) = 4 \times KA \times Y^3 + 3 \times KB \times Y^2 + 2 \times KC \times Y + KD$$

For first approximation Y can be set equal to PD/2

$$\text{so } Y = PD/2$$

This method allows fast and precise calculation with a small number of iterations.

Having Y, one can obtain X and Xo, by substitution.

Consulting Fig. 7, since QP=Xo, distance OP=Xo × tan(q) and roughing zone: Lr=OP - Lg/2

3. ENGAGEMENT ZONE

As mentioned above, the engagement zone is the sum of roughing and generating zones.

$$Le = Lg + Lr$$

The author gratefully acknowledges the assistance of Claude Lutz, American Pfauter Ltd., for technical consulting; Edward P. Driscoll, Driscoll Software Co., for computer analysis; and Frank C. Uherek, Dresser Ind., for article development.

Editors Note: Special thanks to Dennis Gimpert, American Pfauter Ltd., for his technical editing assistance.

E-3 ON READER REPLY CARD

TECHNIQUES FOR ALIGNING & MAINTAINING . . .
(continued from page 43)

APPENDIX A
INSTRUMENTATION SPECIFICATIONS

Surface Contact Pyrometer

A digital type pyrometer having an accuracy of ±3°F and a response time of approximately five seconds or less was used. The contact probe was surrounded by ceramic type substance to shield it from the influence of ambient temperatures.

INFRARED

Instrumentation

There are basically two styles of infrared instruments. One focuses the infrared through a lens and the other reflects it from a mirror. The lens type can be aimed more precisely making it superior from an accuracy viewpoint. Unfortunately, lens type instruments are the least portable.

The specifications of each of these types of infrared instruments can vary widely. The following key specifications are recommended for this application:

Temperature	50°F to 300°F
Spectral Response	8-14 microns
Field of View	2° or less
Spot Size (max.)	1½" at 40" distance
Emissivity Range	.6-1.0 (min. range)

A digital readout or a meter readout with a meter hold feature (not peak) is recommended. Some mirror type instruments are available with laser optics to aid in aiming the instrument. This option makes them equivalent to the lens type.

Setup

Fig. A-1 illustrates the setup of the lens type infrared radiation thermometer. A fluorescent light is an aid for aiming the detector at selected measurement points. It has been determined that the heat emitted from this light does not influence the measurements. It is very important that the light be held horizontally to obtain a horizontal reflection from the pitch line of the mesh. The tripod is recommended.

Fig. A-2 illustrates the setup for a mirror type instrument. In this case, the fluorescent light and tripod are also recommended for instruments without laser sighting optics.

Fig. A-1 – Test Set-Up
Lens Type Infrared Radiation Thermometer

Fig. A-2 – Test Set-Up
Mirror Type Infrared Instrument

E-4 ON READER REPLY CARD

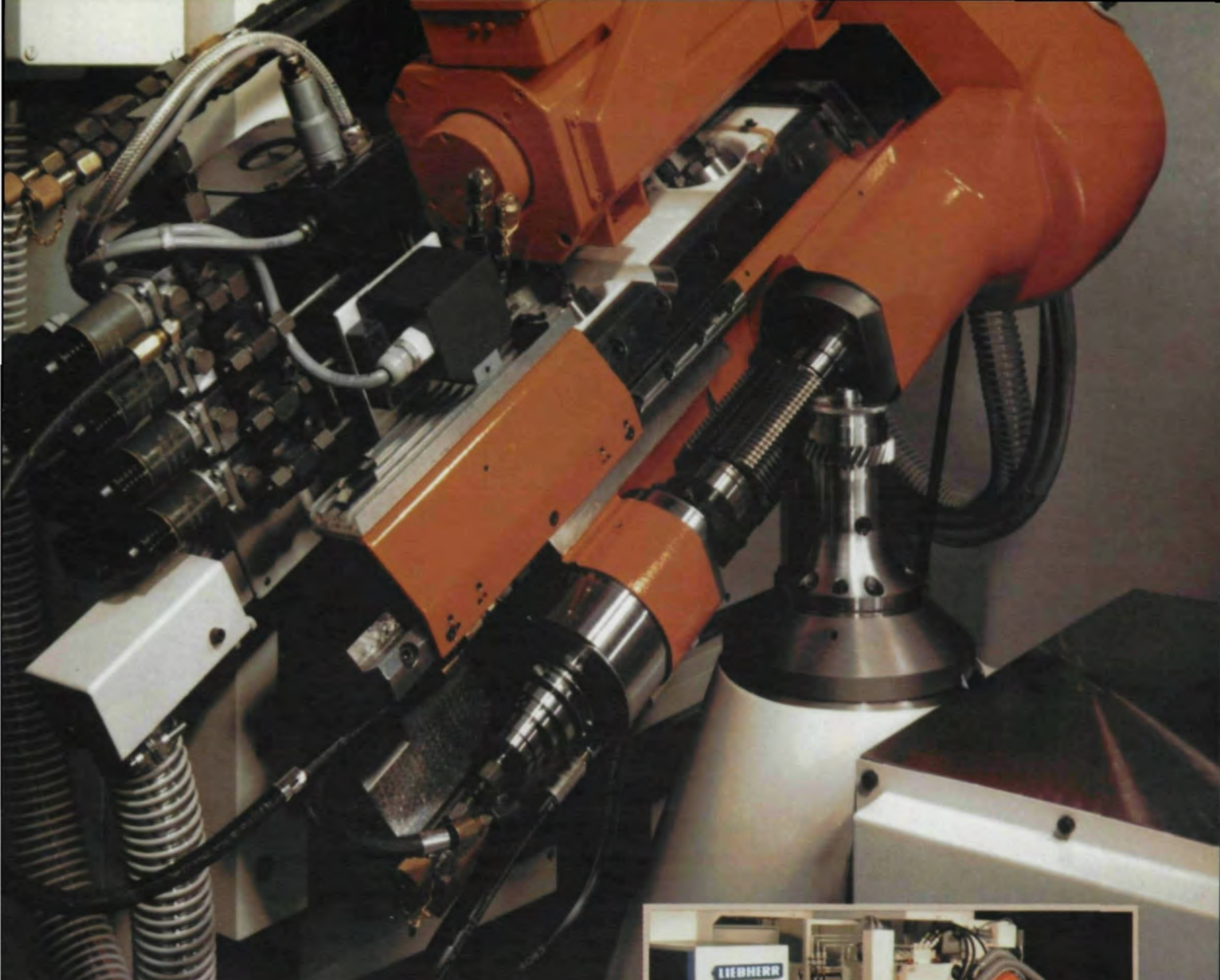

LIEBHERR

We've geared up to give you the edge in gear making

Hard finishing. A process on the cutting edge of metal-working technology. A process that can give you a competitive edge in gear making. And only Gleason gives you a choice of two hard-finishing processes: carbide or CBN cutting—or exclusive CBN grinding.

Hard finishing (using super-hard materials to cut or grind the gear after heat treating) eliminates or greatly reduces process variations and offers significantly higher gear quality: AGMA 12 runout and pitch accuracies, 10–20 microinch CLA finishes (with little or no lapping), more accurate geometry for better load sharing, and less gear noise. You get manufacturing benefits, too: higher production rates, better process control, fewer inspection hours, less scrap, and lower overall cost.

Gleason machines and materials make hard finishing the final process for ultimate quality. The high-precision 643 hypoid grinding machine equipped with CBN grinding wheels is the only hard-finishing grinder on the market. And the 641, 645, 650, 655 and 675 generators deliver the extreme accuracy and rigidity that hard-finish cutting demands. Equipped with Gleason CBN or carbide-tipped cutters, they deliver incomparable results.

Which techniques and machines are the right ones for your operation? You can depend on Gleason to work it out with you. We've been solving gear-making problems for more than 120 years.

Get to know the 600 Series machines—and the new Gleason. For complete hard-finishing information, call 716-473-1000 or write Gleason Works, University Avenue, Rochester, NY 14692, U.S.A.

GLEASON

Advanced concepts, traditional quality.
That's the new Gleason.

CIRCLE A-20 ON READER REPLY CARD